



## **COMPARISON OF SIMULATIONS OF THE TANAWON SECTOR SIMULTANEOUS DISCHARGE TEST IN BACON-MANITO GEOTHERMAL FIELD IN THE PHILIPPINES**

**Kristine Eia S. Antonio**

Energy Development Corporation - EDC  
38/F One Corporate Center Building  
Julia Vargas corner Meralco Avenue  
Ortigas Center, Pasig City, 1605  
PHILIPPINES  
*antonio.kes@energy.com.ph*

### **ABSTRACT**

The Tanawon simultaneous discharge test pressure monitoring data was simulated using lumped parameter, numerical reservoir models, and then with the same models coupled with wellbore simulator HOLA. Ten-year forecasts were run using the various models and the results were compared. The wellbore simulator was used to check whether the wells could produce, assuming the pressure drawdown forecasted by the lumped parameter models. The wellbore simulator was also implicitly coupled with a BGPF numerical reservoir model, which resulted in the extension of the life of the wells in the model due to boiling.

### **1. INTRODUCTION**

Geothermal wells are essential to geothermal research and resource management because they allow access to the resource fluid for study and are the closest measurement points to the reservoir. The testing of geothermal wells or boreholes is, therefore, a vital part of geothermal reservoir management as it provides crucial information regarding the condition of the reservoir (Axelsson, 2013a). Wellbore pressure is one of the first measurements reviewed and analysed by reservoir engineers. Pressure provides information not only about the well that is being measured, but also about the hydrothermal structure of the reservoir (Grant, 1988). Looking at the pressure distribution within a field can provide information on the location of the water table or the existence of flow barriers and resistances throughout the field. Also significant to the reservoir engineer are the pressure changes against time, which can characterize the fluid flow properties that affect a field's production, recharge and, consequently, sustainability. Testing a single well can give knowledge regarding the well's productivity and can be used as a guide for the permeability distribution of the reservoir. Testing multiple wells can produce results which are applicable for a wider area. Ideally, the pressure monitoring data used for sustainability assessment is taken from a well within the producing field over an extended period of time (Bixley, 1988; Ramey, 1988). A type of multi-well test conducted by the Energy Development Corporation (EDC) is a simultaneous discharge test wherein all existing wells in the field being assessed are discharged and the pressure is monitored from one or more shut monitoring wells.

The wellhead pressure, mass flow, enthalpy, and chemistry of the discharging wells are also closely monitored. The objective of simultaneous discharge tests is to study the production capacity of the field in a situation that closely mimics full-scale production. The monitoring data collected during a simultaneous discharge test may be analysed through the use of reservoir models. By calibrating the models against the reservoir pressure and discharge changes through time, the characteristics of the reservoir can be inferred. By simulating long-term production using the calibrated models, the sustainable production level of the field can be estimated from the calculated pressure drawdown and fluid enthalpy in the simulated reservoir. Ironically, most models used to analyse well tests were developed to model the bulk flow through the porous reservoir rocks and the dynamics of the geothermal fluid flowing up the well are simply not part of the modelling process. Pruess (2002) suggested that the interaction of the wellbore and the reservoir be simulated through coupling of a reservoir and wellbore model. This added layer of complexity not only increases computational cost, but requires more data and analysis time to set up. The effect of coupling a wellbore model to a reservoir model must, therefore, be examined.

As a first step in reviewing coupling wellbore and reservoir models, the Tanawon simultaneous discharge test was modelled using standard reservoir models and coupled models. The models were used to forecast 10 years of production and the results of the different forecasts were then compared. The focus of this study is to assess the reservoir modelling techniques used in forecasting and to determine whether incorporating wellbore effects will drastically change the forecast results.

## **2. BACKGROUND OF THE TANAWON SECTOR**

Tanawon is a geographical sector of the Bacon-Manito (BacMan) geothermal production field (BGPF), one of the high-temperature geothermal fields in the Philippines managed by EDC. Tanawon Sector is one of the expansion fields under development, but not yet in full operation in BGPF (EDC, 2013). It is projected to contribute 40 MWe to the geothermal project (DOE, 2013).

### **2.1 Overview of the BacMan resource**

#### **2.1.1 Geologic setting of BacMan**

The Philippines is an archipelagic country that was formed at the convergence of the Sundaland-Eurasia and the Philippine Sea Plates. The country is thus surrounded by subduction zones of various microplates, resulting from the stresses on the deforming major plate boundaries; most related to this study is the Philippine Trench to the east of the country (Figure 1). The Philippine Fault Zone, a left lateral strike slip fault that traverses most of the country in a generally north to south manner, relieves whatever stresses the subduction zones cannot accommodate (Yumul et al., 2008). The presence of many fracture-dominated geothermal reservoirs in the country can be attributed to the main Philippine Fault Zone, its splays, and subsidiary faults (Yumul et al., 2008; Malapitan and Reyes, 2000). The fractures and faults not only provide conduits for hydrothermal fluids, but are also responsible for the intrusion of young plutonics throughout the country. The subduction of the Philippine Sea plate into the Philippine trench is said to be responsible for the magmatism in the East Philippine Volcanic Arc (Yumul et al., 2008) that stretches from the Bicol Peninsula to Mindanao. The East Philippine Volcanic Arc hosts some of the largest geothermal developments in the country, including BGPF (Malapitan and Reyes, 2000).

BGPF is located within the Pocdol volcano or Pocdol Mountains, a cluster of small eruptive craters belonging to the Bicol Belt (EDC, 2003). Like most geothermal systems within the country, the major source of permeability in the BGPF geothermal wells are faults (Malapitan and Reyes, 2000). The major geologic structure in the area is the WNW-ESE trending San Vicente-Linao fault, whose trace cuts

through the Pocdol Mountains as a 5-km wide shear zone dubbed the BacMan fault zone (Figure 2). It is inferred that the San Vicente-Linao fault is a splay of the Philippine fault because the movement of the two faults is related.

Other geologic structures in BGPF follow four major structural trends: WNW-ESE, NW-SE, E-W, and NE-SW. The NW-SE trending structures, labelled the Pocdol belt (Figure 2), are said to control the deep south-eastward flow of geothermal fluids (EDC, 2003; Braganza, 2011).

The development area of BGPF is located within the intersection of the BacMan fault zone and the Pocdol belt (Braganza, 2011). While the most recent volcanic activity in the Pocdol Mountains is estimated to have occurred 40,000 years ago. Reyes et al. (1995) used the presence of kaipohans - ground discharge of  $H_2S$  and  $CO_2$  that are related to high-temperature hydrothermal systems with an acidic core - and solfataras in rugged terrains as evidence of a young heat source. The subsurface stratigraphy of the field as derived from well cuttings is divided into the Late Pliocene-Late Pleistocene Pocdol volcanics and the Late Miocene-Early Pliocene Gayong sedimentary formation (Ramos, 2002).

### 2.1.2 BacMan resource and development

BGPF was one of the geothermal prospects identified by the Commission on Volcanology (COMVOL) in the 1970s and is one of the actively producing geothermal projects in the country. Logistically, the main production field can be divided into two developmental units: the Palayang Bayan sector, which supplies steam to the 110 MWe BacMan I turbines, and all other fields outside of the Palayang Bayan sector, collectively known as BacMan II. The development of BGPF began with an initial geoscientific exploration study in September, 1977 with shallow depth vertical electrical soundings, semi-detailed geological mapping, detailed geochemical investigations, and, eventually, the drilling of medium-depth exploration wells Manito 1 and 2 (Tolentino and Alcaraz, 1986). BacMan I was eventually

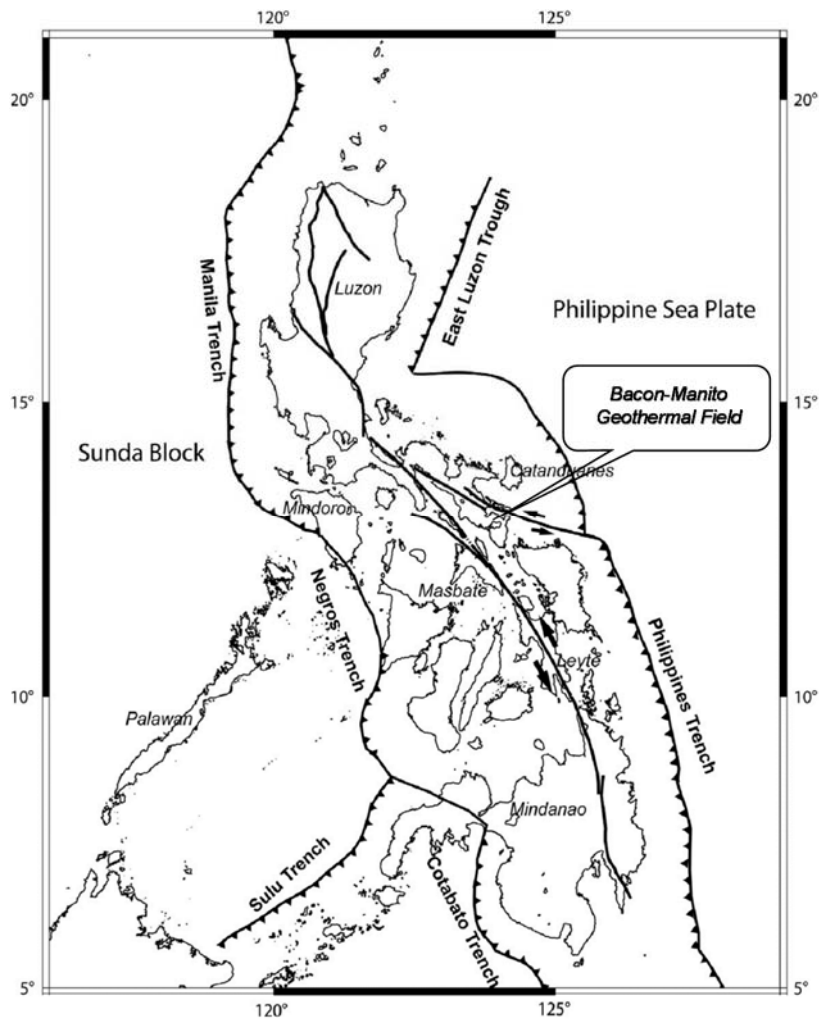


FIGURE 1: BGPF Location on Philippine tectonic setting map (modified from Yu, et al., 2013)

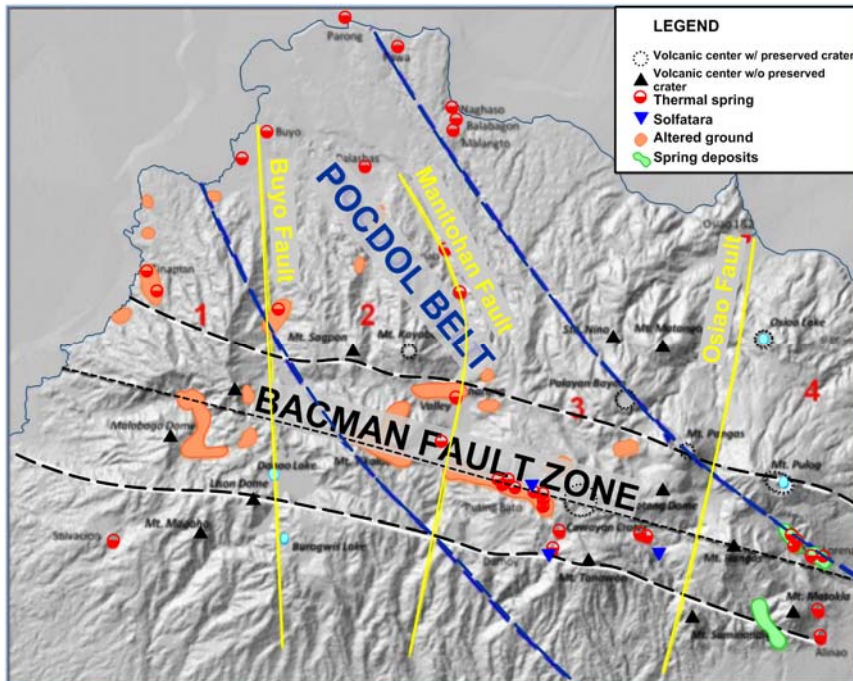


FIGURE 2: BGPF relief contrasts showing the BacMan fault zone (black) and Pocdol belt (blue) (modified from Braganza, 2011)

commissioned in 1993, Cawayan in 1994, and Botong in 1998. To date, BacMan II has two 20 MWe turbines commissioned, one each for Botong and Cawayan sectors. Based on the Philippine Department of Energy list of private sector initiated power projects, as of 12 August 2013, three additional power projects in Tanawon, Rangas, and Kayabon sectors have been indicated for BacMan II at 40 MWe each. All projects are undergoing feasibility studies. Tanawon has a target commissioning date on December 2018, while Rangas and Kayabon are aiming to be commissioned by 2019 (DOE, 2013).

The latest hydrogeological model of the BacMan resource puts the main upflow of the field beneath Palayang Bayan and Botong where the highest temperatures have been found (Ramos and Santos, 2012). The high temperatures exceeding 300°C that are indicated by a closed isothermal contour of secondary biotite (Ramos and Santos, 2012) are corroborated by both measured temperatures (Austria, 2008) and quartz temperatures (Ruaya, et al., 1994) in wells drilled in the general direction of the upflow (Figure 3). The preferential outflow direction is towards the northwest where the 240-280°C isothermal contours based on hydrothermal alteration dip gently (Ramos and Santos, 2012). The elongation of T-quartz temperature contours towards Inang Maharang indicates the same preferred outflow direction (Ruaya, et al., 1994). Exploration well IM-1 and the injection wells in the Inang Maharang region exhibit a downflowing profile which is typical of wells drilled along resource boundaries (Austria, 2008). A minor outflow is directed towards Rangas in the southeast. Steeply dipping isotherms based on hydrothermal alterations and a high pressure anomaly northeast of Palayang Bayan suggest a geologic boundary that acts as a flow barrier from the main field to the Osiao-Pangas-Botong area (Ramos

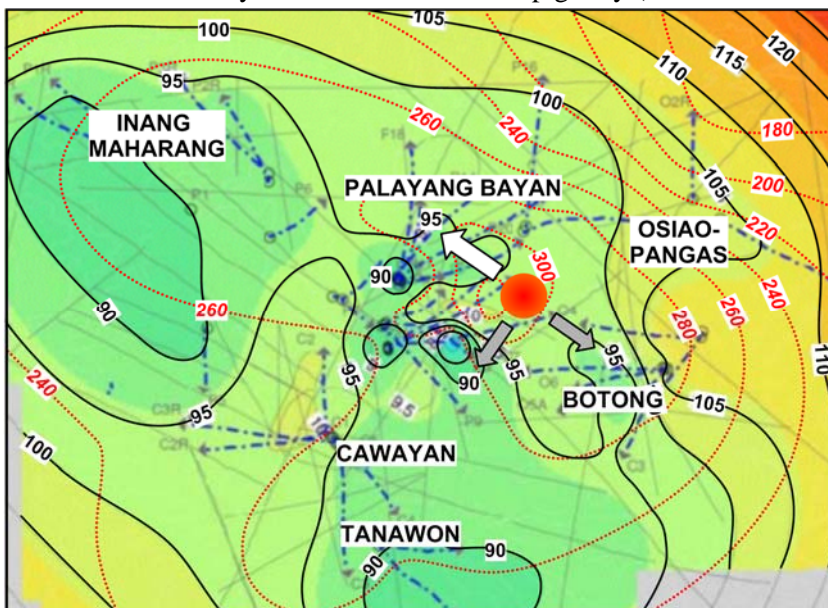


FIGURE 3: BGPF pressure (solid, black) and temperature contours (dotted, red) (modified from Austria, 2008)

and Santos, 2012). The elongation of T-quartz temperature contours towards Inang Maharang indicates the same preferred outflow direction (Ruaya, et al., 1994). Exploration well IM-1 and the injection wells in the Inang Maharang region exhibit a downflowing profile which is typical of wells drilled along resource boundaries (Austria, 2008). A minor outflow is directed towards Rangas in the southeast. Steeply dipping isotherms based on hydrothermal alterations and a high pressure anomaly northeast of Palayang Bayan suggest a geologic boundary that acts as a flow barrier from the main field to the Osiao-Pangas-Botong area (Ramos

and Santos, 2012; Austria, 2008). A third outflow is towards the southwest to Cawayan and then Tanawon. The existence of a minor localized upflow in the Cawayan area was also suggested on the basis of fluid inclusion studies (Reyes, et al., 1995). The latest data from drilling have shown a low-temperature gradient and poor permeability associated with fine-grained clastics towards the southwest of Tanawon, possibly demarcating the boundary of the BacMan resource in that direction (Ramos and Santos, 2012).

Austria's 2008 resource assessment of BGPF, a volumetric assessment, shows a 90% probability of BacMan I producing 94.1 MWe and BacMan II producing 106.3 MWe from 2006 to 2031, while dynamic modelling techniques indicated that BacMan I and BacMan II combined can sustainably produce 150 MWe.

## 2.2 Brief history of Tanawon sector development

The Tanawon sector is at the periphery of the BacMan resource and is located within a high resistivity block identified during the initial geoscientific studies of the area. Interest in the sector began after the drilling of Well CN3D in 1990. Well CN3D was originally meant to be a reinjection well drilled within sector C of the BacMan field (Figure 4). It was converted to a production well due to its good permeability, productivity, and temperatures reaching 270°C. The results of drilling Well CN3D led to the recontouring of the resource boundaries and the addition of resource blocks I and K. Resource block I is an extension of the Cawayan resource block while resource block K is the Tanawon sector (Figure 4). Thus, development in the Tanawon field is fairly recent in comparison to the developmental history of BGPF, which started commercial operation in 1993; its main production area is within 2 km south of the production area of the Cawayan sector whose 20 MWe plant was commissioned in 1994.

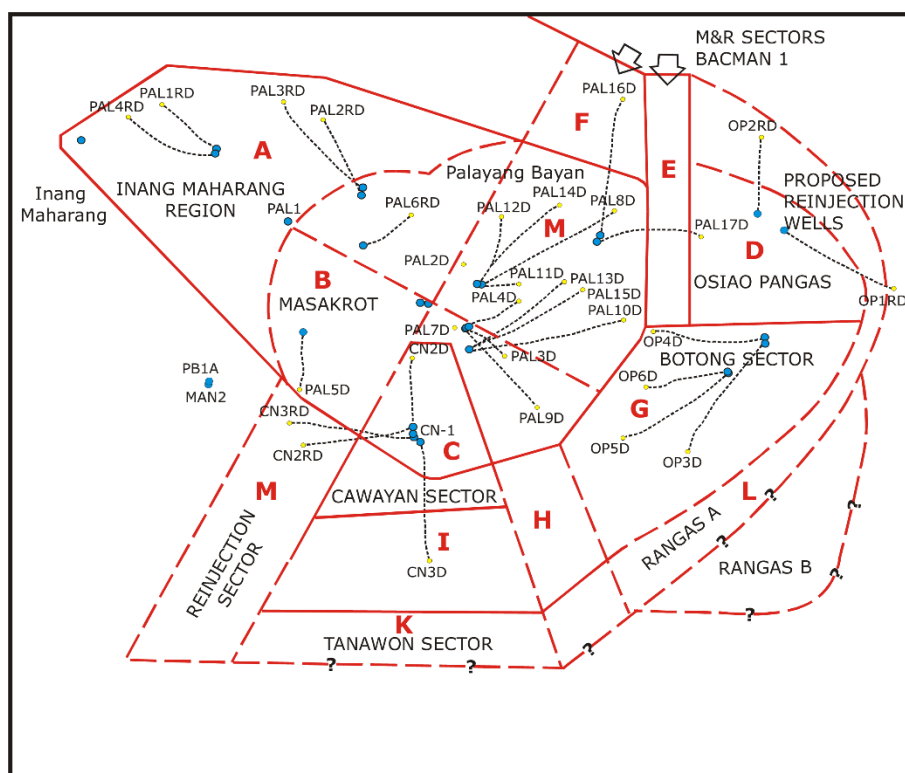


FIGURE 4: BGPF Sectors (from EDC, 2003)

Initial drilling in Tanawon sector started in 2000 with two directional wells: Well TW-1D (2050.5 mMD) and Well TW-2D (2611.8 mMD) (Fajardo and Malate, 2005). Additional production wells and one reinjection well have since been drilled in the sector between 2011 and 2012.

### 2.3 Tanawon simultaneous discharge test

The simultaneous discharge test was conducted to gain an understanding about the possible response of the Tanawon field to full production. Three production wells within the Tanawon field, Wells TW-1D, TW-2D, and TW-4D, were simultaneously allowed to discharge while pressure response was monitored from monitoring Well TW-3DA using a Pruett-type tool (Pruett, 2013). The main objectives of the test were to determine the steam available, the behaviour of the discharging and nearby wells, monitor possible changes in the physical and chemical properties of the discharge fluid, and obtain additional data for Tanawon resource assessment. Pressure monitoring data is available for most of the test except for a break from day 79 to 107 while the tool was being recalibrated after the retrieved data for the preceding 15 days proved to be erratic. The discharge of the wells in Tanawon was monitored using the James lip pressure method (Grant, 1982).

The goal was to discharge the wells at full capacity throughout the discharge test period; however, due to the deteriorating reinjection capacity of Tanawon's reinjection well, Wells TW-1D and TW-4D were shut from days 59 to 66. Due to reinjection issues, Well TW-4D was often throttled to maintain the wellhead pressure in the reinjection well. Wells TW-1D and TW-4D were eventually shut on the 179th day. All Tanawon wells were closed on the 209th day. Pressure monitoring continued until the 229th day to recover pressure lost during the shutdown of the field. Figure 5 illustrates the pressure trends against the significant events during the simultaneous discharge.

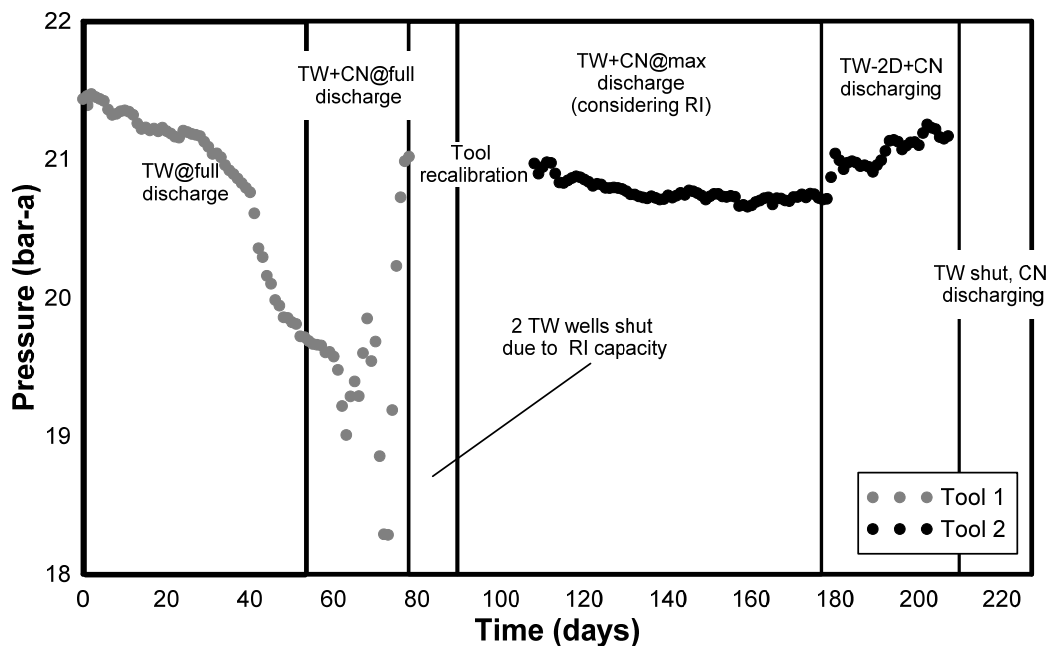


FIGURE 5: Simultaneous discharge test: average daily pressure measurements with annotations

Because an intimate connection between Tanawon and Cawayan had been observed, during the Tanawon discharge test, Cawayan was also monitored. To ensure that the behaviour captured was as close as possible to actual production behaviour, Cawayan was discharged at its full load of 20 MWe from day 55 to the end of the test. BacMan I was also kept under production throughout the test.

### 3. MODELLING IN GEOTHERMAL SYSTEMS

The mathematical modelling of the different aspects of geothermal systems has become a standard analysis technique in the study of geothermal reservoirs. Most models have a two-fold purpose: first to characterize the system being modelled and second to predict the response of the system to changes in utilization (Axelsson, 2013b). Two aspects that can be modelled in geothermal systems are the geothermal reservoir and the geothermal wellbore. Geothermal reservoir models describe the resource and can be used to characterize the reservoir rock while geothermal wellbore models describe the flow up the wellbore pipe and the portion of the reservoir feeding fluid into the wellbore. While the wellbore and the reservoir are closely connected and deal with the same fluid, because of the difference in the flow equations and time-scale involved, they are often modelled separately.

#### 3.1 Reservoir modelling

Geothermal reservoir models can be used to quantify reservoir parameters and forecast reservoir response and output based on a given utilization scenario. Reservoir models have been used extensively throughout the geothermal industry as part of resource management. Models range from simple heat in place models based on the area of the resource to complex numerical reservoir models. In 2001, an informal survey by O'Sullivan et al. (2001) found that there are over a hundred geothermal fields with developed reservoir models. Two years later, Pruess (2003) put the number at several hundred fields. The growing number of fields utilizing geothermal reservoir models stresses the importance of geothermal reservoir modelling to project development.

There are several reservoir modelling techniques available for geothermal reservoir assessment and the modelling technique to be used should be determined by the availability of data and the objective of the modelling study (Axelsson, 1989). There are two main categories of modelling techniques used in the geothermal industry. Static modelling techniques use the amount of heat contained by the reservoir to estimate the output without taking into account changes in time; while dynamic modelling techniques look at the nature and response of the geothermal reservoir to disturbances due to utilization and exploitation and the corresponding output of the reservoir based on these (Axelsson, 2013b).

The list of the main modelling methods below was adapted from Axelsson (2013b):

##### Static modelling techniques

- Deep temperature estimates
- Surface thermal flux
- Volumetric method

##### Simple dynamic modelling techniques

- Decline curve analysis
- Simple mathematical modelling
- Lumped parameter modelling
- Detailed numerical modelling

The principal static modelling method is the volumetric method (Axelsson, 2013b). The volumetric method is used when surface data is available. Volumetric methods use the least subsurface information and thus have the greatest amount of uncertain, albeit educated, assumptions. Unfortunately, it is rare that sufficient subsurface data is available at the stage of geothermal development where financial commitments are obtained. Grant (1997) makes the point that initial resource assessments are often extremely optimistic, not because of calculation errors, but because of changes in the understanding of the reservoir being assessed. The output of such assessments should, therefore, be presented in such a way that explicitly recognizes the presence of such uncertainty. For this reason, the volumetric method is often coupled with a Monte Carlo simulation that can create a probability distribution of reservoir outputs.

The principal methods of dynamic modelling can be further subdivided into simple dynamic modelling techniques and the detailed numerical reservoir models. Simple models do not consider or reduce the spatial heterogeneity and variations in response of the reservoir in order to obtain a closed analytic form that describes the reservoir response. The lumped parameter modelling of water level or pressure changes is the principal simple dynamic method for studying the long-term response of low-temperature geothermal systems to utilization (Axelsson, 2013b). The Theis model is another simple mathematical model which is extensively used, but mostly for analysis of geothermal well tests which are on a much shorter time scale than a full production history. Detailed numerical models, in contrast to simple models, attempt to represent the geometry and spatial heterogeneity of the reservoir and determine the response of the reservoir through calculating the flow of fluid and heat through it. Numerical models require a significant amount of time and data for set up and calibration, but a model with sufficient detail can be instrumental in studying the physical and chemical processes that control the behaviour of the geothermal system (Axelsson, 2013b).

### 3.1.1 Lumped parameter models

Lumped parameter modelling of geothermal systems simplifies the geothermal system as a network of tanks and fluid conductors. Each tank in the network is characterized by a storage coefficient,  $\kappa$ , such that when liquid of mass  $m$  is injected into the tank, the pressure in the tank is the response  $p = m/\kappa$ . Pairs of tanks are connected by conductors which are described by conductance,  $\sigma$ , which transmits a mass flow  $q = \sigma \nabla P$  where  $\nabla P$  is the pressure difference between the tanks. Flow between tanks is always from the tank with a higher pressure to the tank with a lower pressure. The network can be modelled as either closed where flows are only between tanks and there is no external recharge or open wherein the network is connected to a constant pressure infinite source analogous to an electrical ground which acts as a recharge boundary. The derivation of the analytical solution to this problem is detailed by Axelsson (1989).

The main problem when performing lumped parameter modelling is the calculation of the tank and conductor parameters. LUMPFIT is a program that automates this calculation by treating it as an inverse modelling problem. For simplicity, fluid extraction or injection is limited to one tank which represents the main production or injection field. Pressure monitoring is also assumed to be within this tank. The pressure response in an  $N$ -tank system is given by

$$p(t) = - \sum_{j=1}^N Q(t) \frac{A_j}{L_j} (1 - e^{-L_j t}) - Q(t) B t \quad (1)$$

where  $A_j$ ,  $L_j$ , and  $B$  are functions of the corresponding  $\kappa$ 's and  $\sigma$ 's.

Assuming a constant production,  $Q$ , pressure response of the tank would be declining. The magnitude of the lowering pressure is controlled by the amplitude coefficient,  $A$ 's while the  $L$ 's coefficient most strongly influences the rate of decay over time. Parameter  $B$  introduces boundary conditions wherein a closed system with no recharge would have a linear pressure decline over time for constant production. For an open system with recharge,  $B = 0$ , meaning the pressure in the tank would eventually stabilize (Axelsson and Arason, 1992).

Axelsson et al. (2005) presented cases from Iceland wherein the results of lumped parameter modelling were validated against actual monitoring data. It was found that the models were quite reliable and that the actual pressure response was expected to fall between the open and closed model forecasts. One of the goals of using lumped parameter modelling is, therefore, to find an optimistic open model and a pessimistic closed model (Liu, 2011).

Other significant findings during this validation process are that the most reliable models were those based on a long production history and that uncertainty in predictions increased with an increasing



forecasting period. As a final note, it was stressed that lumped parameter modelling assumes isothermal single-phase conditions and that changes in reservoir conditions such as boiling and changes in reservoir properties such as an increase in permeability due to seismic activity could make the results unreliable (Axelsson et al., 2005).

### 3.1.2 Numerical reservoir models

Detailed numerical reservoir models are one of the most powerful tools for studying geothermal reservoirs and numerical modelling has been a standard practice since the 1990s. The main steps of developing a geothermal reservoir model have been established and the list below was adapted from Axelsson (2013b):

- Dividing the reservoir into small semi-homogenous sub-volumes called grid-blocks;
- Assigning hydrological and thermal properties to the grid-blocks;
- Adding sources to represent fluid and heat entering the reservoir and sinks to represent fluid and heat exiting the reservoir; and
- Specifying appropriate boundary conditions.

Assigning grid-block properties can be a time consuming process and requires a well-developed conceptual model that describes the location of the upflowing heat and fluid source, the flow paths of the fluids, and the exit points from the field or outflows. The grid-block properties must be consistent with the conceptual model and produce flows that are consistent with well test data. The calibration process of finding the appropriate grid-block properties is a two-step process which involves natural state modelling followed by matching production history. Natural state modelling allows the model to evolve over geologic model time until the pre-exploitation temperature and pressures of the reservoir are matched. Production state matching, on the other hand, involves matching the measured response of wells to the production such as pressure drawdown and enthalpy and mass flow trends. These two steps, though often called stages of model calibration, are an iterative process of adjustments made to the grid-block properties, which if done during the production history matching phase should cause a deterioration of the matches made with the natural state model. Today, the calibration process has been made more efficient by the development of inverse modelling software such as iTOUGH2 and PEST; but, even with such technologies, the most complex reservoir models can take a long time to calibrate.

Setting up the boundary conditions is another part of the calibration process. The model can cover only a finite area, but its boundaries must be set so as not to affect the main reservoir. In many cases, this involves setting up very large grids that encompass an area much larger than the actual geothermal field being modelled. The large grids required for such simulations often lead to large grid-blocks, which are not suitable for capturing the behaviour of flow within fractures or through wells. For geothermal systems, flow through fractures are often dominant, and many solutions to the large grid-block sizes have been put forward, including dual-porosity models, process models, and sub-grids.

O'Sullivan et al. (2001) opined that the technology of geothermal reservoir modelling was already mature during the early 2000s. Despite borrowing and adapting many technologies and techniques from groundwater and oil and gas modelling, geothermal reservoir engineering lagged behind its counterparts in related industries because geothermal systems tend to involve multiphase and multi-component fluids moving in a highly heterogeneous environment. While there are numerous multiphase-multi-component simulators available, their capabilities are often limited compared to the problem they need to solve. In addition to this, as geothermal technology evolves, so do the requirements of the reservoir models. Modelling of enhanced geothermal systems, for example, requires modelling of dynamic changes in fracture permeability which most hydrothermal modelling software cannot easily simulate. In the recent past, the primary barrier to the development of numerical models was the amount of computing power that was available, making simulation time and the calibration process prohibitive. Today, this barrier is being overcome both by advancement in computing technology and in development of more efficient

computing algorithms; the current trend of geothermal reservoir modelling, therefore, is to create a fully-coupled thermo-hydro-mechanical-chemical simulation code for the reservoir itself (IPGT, 2012).

### 3.2 Wellbore modelling

Geothermal wellbore models are flow within pipe models that can be used to assess how fluids flow in from the reservoir and subsequently travel up the wellbore. In wellbore models, fluids enter the well through localized productive zones called feedzones. The highly localized inflow is common in wells that are drilled through fractured volcanic rocks of low porosity (Björnsson, 1987) where fluid flows are mainly through fractures. Flow properties are calculated given pressure conditions either at the wellhead or at the feedzone depth. Properly set-up models can be used to estimate the change in the output of the well with variations in wellbore and reservoir conditions.

Wellbore models are comprised of two main parts: the wellbore geometry and the feedzone properties. The most basic wellbore geometry describes the configuration of the well via the well depth and the inner diameter of the casings and liners or open hole. Some simulators allow for deviated wells and, thus, the location of the kick-off point and the deviation angle are also used. Feedzones also need to be described by their mass flow contribution,  $q$ , and enthalpy. The mass flow contribution may be provided either as productivity and reservoir pressure or a fixed mass flow. The productivity of a feedzone is often given as a productivity index,  $PI$  (Equation 2), which is a proportionality constant relating the mass flow contribution of a feedzone and the pressure difference,  $\Delta P$ , between the wellbore at the feedzone depth and the reservoir.

$$PI = \frac{q}{\Delta P} \quad (2)$$

The more advanced wellbore simulators also consider dissolved salts and  $\text{CO}_2$ . Wellbore simulators can be run either from the top down to the deepest feedzone, in which case the wellhead pressure, enthalpy, and mass flow need to be supplied to the simulator; or from the deepest feedzone to the wellhead, in which case the wellbore pressure at the deepest feedzone is needed. Wellbore models that use productivity indices can be used to create bore output curves by running the model with varying deepest feedzone wellbore pressures. Figure 6 shows an example of a wellbore profile calculated by HOLA.

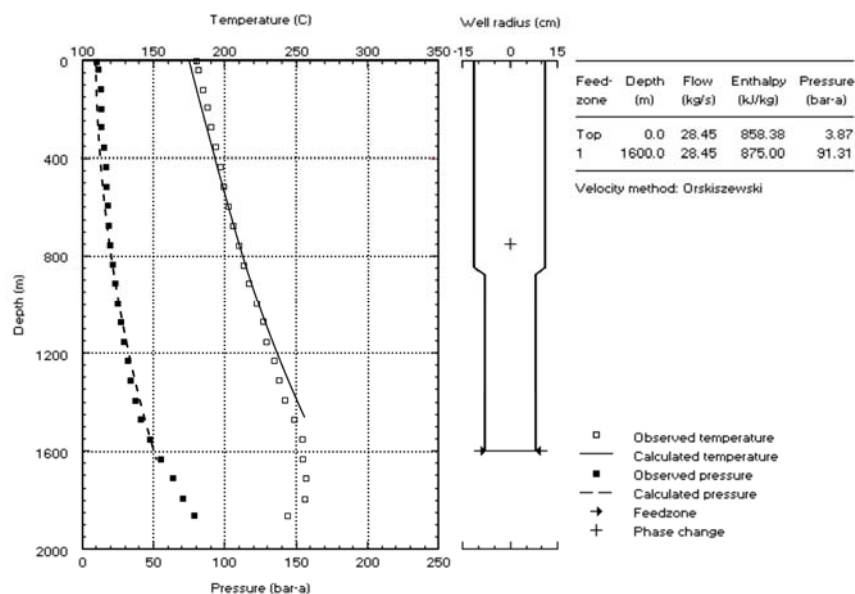


FIGURE 6: HOLA wellbore model example

Figure 6 shows an example of a wellbore profile calculated by HOLA.

Accurate wellbore geometry is sometimes easily obtained from the drilling information; but, in many cases, wells have blockages, scaling, or thinning. Blockage surveys or multi-finger caliper surveys will provide useful information, though often the modeller has to make assumptions about the length of the affected section and its diameter. Creating a wellbore geometry that is as close as possible to reality is important because the pressure drop from the feedzone to the wellhead is significantly affected by this.

Calibration of feedzone properties involves matching discharge pressure and temperature profiles of wells at a corresponding mass flow. If the information is available, relative velocity profiles can also be matched. Accurate wellhead parameters are, therefore, important in this part of the process. For various reasons, it is not unusual to find that the wellhead pressure read from the wellhead is not consistent with the 0-depth pressure read by the pressure survey tool. The modeller will, therefore, have to make assumptions regarding the correct wellhead pressure, mass flow, and enthalpy.

Freeston and Gunn (1993) observed that wellbore simulations have also become important not only as a tool to optimize the utilization of wellbores, but also as a means to improve reservoir models. Wellbore modelling can be used to gain insights on the optimum well design, determining minimum wellhead pressure that would prevent scaling in the casing (Björnsson, 1987), estimating improvements after acidizing (Fajardo and Malate, 2005) or clearing, and gauging the effects of drawdown. Aragon et al. (1999) stated that when calibrated correctly, wellbore simulations can sometimes reduce the need for Pressure-Temperature-Mass Flow (PTQ) logs, which are most often used to determine the distribution of mass flow contributions amongst feedzones. While most wellbore simulators are steady state simulators that assume stabilized discharge, there are transient wellbore simulators available.

### 3.3 Coupling of reservoir and wellbore models

Representing wellbore flow within a reservoir model has long been a subject of computational studies. Though simplified well “models” are included in most reservoir simulators in the form of mass sinks, the complexity of the two-phase flow inside the well is ignored (Murray and Gunn, 1993). The reservoir model limitations that are addressed by considering wellbore flow in reservoir simulations include ensuring that the mass extracted from the reservoir reaches the surface with sufficient wellhead pressure, interaction between the different feedzones of the well, and possibly simulating reduced discharge capability of a well that is wellbore-related and not reservoir related as in the case of blockages.

Many methods have been proposed in order to perform this task and these methods can be divided into two groups: methods that integrate wellbore flow into the model, and methods that couple a wellbore simulator with a reservoir simulator. Some examples of wellbore models integrated into a wellbore simulator are the T2Well module for TOUGH2 (Pan and Oldenburg, 2012), the work of Marcolini and Battistelli (2012), and the work of Hu et al. (2007). Developing the integrated wellbore and reservoir simulators involves adding to or changing the code of the reservoir simulator, as in the case of Pan and Oldenburg and Marcolini and Battistelli or programming a new simulator altogether as did Hu et al. Coupling of simulators, on the other hand, utilizes existing simulators and linking them by feeding the outputs of one as inputs to the other. This input-output cycle can be done either explicitly or separately through the creation of well tables.

Explicitly coupling a wellbore simulator and a reservoir simulator is the most straightforward approach to including wellbore effects into a reservoir simulation (Pruess, 2002). Murray and Gunn (1993) credit Hadgu et al. (2007) for the first explicit coupling of a wellbore simulator and reservoir model. This study linked Hadgu’s WFSa wellbore simulator with a TOUGH reservoir model. The modeller provided the required wellhead pressure and wellbore geometry, TOUGH supplied reservoir properties such as reservoir pressure and fluid enthalpy required by WFSa, and WFSa would iterate over different wellbore pressures until the required wellhead pressure was matched (Murray and Gunn, 1993). More recently, Rivera (2010) coupled HOLA with TOUGH2 using shell scripts, and Gudmundsdóttir (2012) coupled FloWell with TOUGH2 via iTOUGH2-PEST.

One approach that is fairly simple to implement is coupling simulators via well tables. Assuming a fixed wellhead pressure, the wellbore pressure at a feedzone required to discharge the fluid at this wellhead pressure would be a function of mass flow and enthalpy. A well table would give the required wellbore pressure at the feedzone of the well given a specific mass flow and enthalpy pair. Creating a well table involves running the wellbore simulator repeatedly over varying mass flow and enthalpy

conditions. The reservoir simulator would then interpolate using the well tables as to which wellbore pressure it would give a well, provided the enthalpy of the block. Well tables are a facility of certain reservoir simulators such as TOUGH2 and TETRAD.

#### **4. HOLA WELLBORE MODELS OF TANAWON WELLS**

As part of the study of the discharge properties of the Tanawon wells, Pressure-Temperature-Spinner profiles of Wells TW-2D and TW-4D were taken. Well TW-1D was not surveyed due to a shallow blockage, but an older discharge profile was available. In order to determine the productivity indices of the wells, calibrated wellbore models were developed using HOLA wellbore simulator to match the discharge profiles of the Tanawon wells. From the wellbore models, the productivity indices and wellbore pressures at the feedzone were derived and incorporated into the AUTOUGH2 input file of the BacMan reservoir model.

##### **4.1 HOLA wellbore simulator**

The earliest version of wellbore simulator HOLA was developed and validated by Björnsson in 1987 as a “Multi-Feedzone Geothermal Wellbore Simulator”. The simulator treats the flow within the wellbore as a one-dimensional steady state flow within a vertical pipe. The pipe is thus divided into a series of grid points and HOLA solves the mass, momentum, and energy flow through the pipe using an explicit finite difference method. The fluid inside the wellbore is assumed to be pure water, but it can occur as a two-phase fluid. To calculate the flow of the two-phase fluid, HOLA uses the method of separated flow models which calculates the flow of the steam and liquid separately, then correlates the two using phase velocity correlations, which have been empirically derived (Björnsson, 1987).

HOLA allows for modelling of multiple feedzones inside the wellbore and each feedzone is modelled as a feed point that is located on one of the grid points (Björnsson, 1987). The feed point properties that are required by the simulator are depth, enthalpy, reservoir pressure at the depth of the feed point, and a productivity index.

The HOLA version used in this study is HOLA version 3.3 compiled in September 1994. This version allows for six simulation modes. The mode most utilized for this study was mode 2 which finds discharge profiles for a required wellhead pressure given the feed point properties. Mode 2 varies the pressure at the deepest feed point until a pre-defined wellhead pressure is achieved. Four-phase velocity methods can be used: Armand, Orkiszewski, Chisholm, and Björnsson. All simulations in this work were done using the Orkiszewski correlation. Though based on empirical behaviour of oil and gas wells, the use of the Orkiszewski correlation for geothermal wells was recommended in the early days of geothermal wellbore simulators. In a pair of companion papers by Ambastha and Gudmundsson (1986a; 1986b) it was demonstrated by matching the flow in the production casing that the Orkiszewski correlation has a general applicability for modelling geothermal wellbore flow and good matches between the measured and calculated pressures and temperatures were obtained, particularly if the steam mass flux was above  $100 \text{ kg/s-m}^2$  (Ambastha and Gudmundsson, 1986a). Further research regarding flow correlations was recommended by the authors as flow within the slug regime was not well matched (Ambastha and Gudmundsson, 1986b). Since the development of HOLA, new flow correlations have been developed and utilized in other wellbore simulators. The flow correlation is an important part of geothermal wellbore modelling because the pressure loss due to friction is strongly determined by the flow adjacent to the walls of the well, which is a matter dictated by the flow correlation used (Hsu and Graham, 1976).

## 4.2 Tanawon wellbore models

The three Tanawon wells that were modelled were Wells TW-1D, TW-2D, and TW-4D. Two models were created for each well. The base model is a multi-feed zone model which attempts to match the behaviour of the well. This base model is used to select the feedzone that contributes the most to the overall mass flow of the well. A single feedzone “TOUGH Model” is then constructed by selecting the depth in the wellbore model closest to the major feedzone that has a corresponding block centre in the AUTOUGH2 model.

Wells TW-1D and TW-2D were drilled in 2000 through a joint venture of Kyushu Electric Power Company of Japan and PNO-EDC. The drilling of both wells suffered persistent fills, tight spots, stuck pipes and eventually premature termination. Post-drilling well tests suggested formation damage as indicated by positive skin and this was attributed to large amounts of viscous mud lost-in-hole and cement injected into the formation through cement plugging. The wells were thus given acid treatment to cure the formation damage (Fajardo and Malate, 2005).

Well TW-1D is a standard diameter wellbore. Its stable discharge at fully opened conditions has a discharge enthalpy of 1400 kJ/kg while throttling the well brings the enthalpy to about 1200 kJ/kg. The difference in enthalpy is attributed to flashing in the formation, resulting from significant pressure drawdown caused by large mass extractions (Fajardo and Malate, 2005).

The base line model for Well TW-1D is a two feedzone model based on a throttled condition survey done in 2001. The feedzones are a liquid enthalpy, low productivity feed at the bottom to model the observed temperature inversion, and a higher productivity index feedzone 100 m from the bottom. The base model matched the pressure slightly better than the temperature (Figure 7). The calculated temperatures tended to be slightly higher than the measured values, with a maximum deviation of +2°C close to the wellhead. The temperature trend at the bottom was also not well captured as the calculated temperature showed a step change while the measured temperatures had a more gradual change. The largest temperature deviation from measured temperatures of -18°C occurred near the bottom of the well between the two simulated feedzones. The feedzone depth in the TOUGH model is set between the feedzones of the base model and given an enthalpy closer to the major feedzone enthalpy. The TOUGH model overlaps with the base model except at its bottom where the base model only has low enthalpy flow from its deepest feedzone.

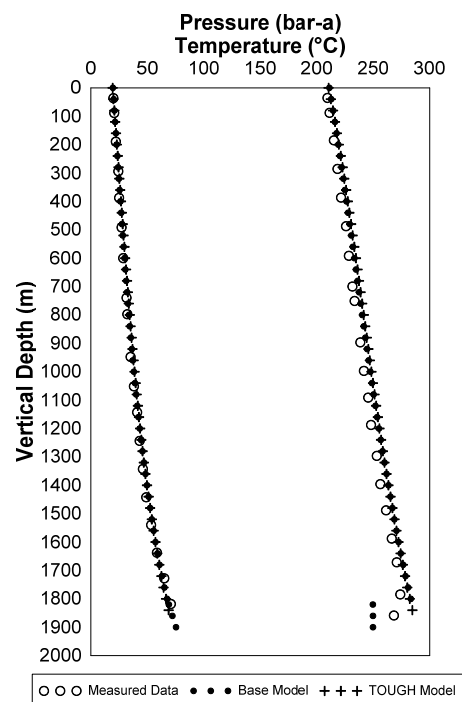


FIGURE 7: Well TW-1D discharge profile

Well TW-2D was drilled as a large diameter well in the hopes of overcoming the drilling problems encountered by Well TW-1D (Fajardo and Malate, 2005). The discharge characteristics of Well TW-2D were low enthalpy of about 1090 kJ/kg. Fully open discharge mass flow and wellhead pressure were also lower than in Well TW-1D.

The base model of Well TW-2D was calibrated against the throttled condition profile because HOLA could not calculate a discharge profile for the fully-opened condition, which had a low wellhead pressure (Figure 8). The base model for Well TW-2D was similar to the base model of Well TW-1D, and had a low enthalpy, low productivity feedzone at the bottom and a higher enthalpy, higher productivity feedzone 100 m above the bottom. In order to match the discharge profile, measured enthalpy at the wellhead was adjusted by +50 kJ/kg. This shift in enthalpy was necessary to discharge the well in

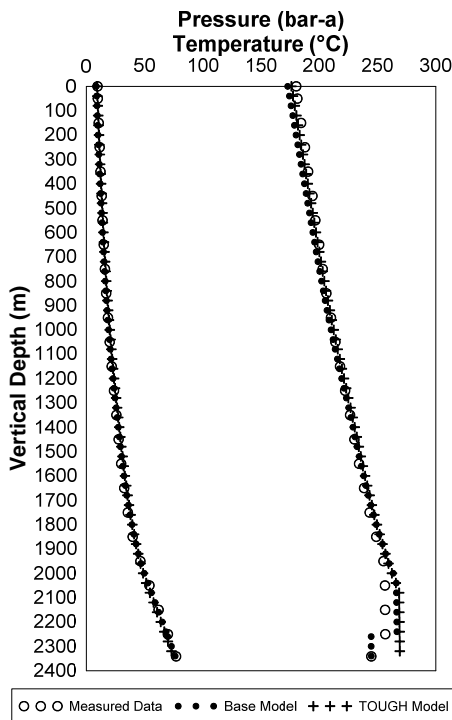


FIGURE 8: Well TW-2D discharge profiles

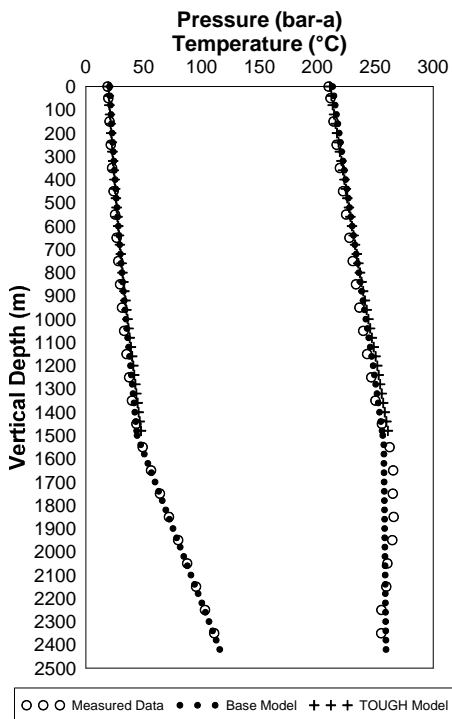


FIGURE 9: Well TW-4D discharge profiles

HOLA, which was calculating a too large pressure drop and consequently choking the well when the measured enthalpy was used. It was the same as Well TW-1D; the TOUGH model feedzone was set between the two base model feedzones.

Well TW-4D was recently drilled, designed to be a large diameter well. Drilling problems encountered during its drilling led to a configuration that is similar to a large diameter well at the top, but then tapers to a standard well at the bottom, resulting in a hybrid configuration. After drilling, Well TW-4D underwent a stimulation programme that involved perforation of its blank liner and acidizing it. The discharge characteristics of Well TW-4D are similar to the discharge characteristics of Well TW-1D, albeit at a higher enthalpy even when throttled. The higher enthalpy of Well TW-4D is attributed to the feedzones from its perforated section which is shallower.

The base model of Well TW-4D puts the major feed at the perforated section of the well, which is consistent with findings from spinner surveys. The match between the base model and the measured data is good for pressure and acceptable for temperature (Figure 9). A better match for the temperature profile can be made by adding more feedzones, but for the purpose of identifying the major zones in the well, it was deemed unnecessary. The enthalpy at this feedzone was set to 1400 kJ/kg.

In modelling the Tanawon wells, some compromises had to be made to work around some of the limitations of HOLA. First off, the Tanawon wells are all deviated wells and had to be converted to vertical wells. This led to a shorter pipe because the vertical depths of the wells were used instead of the measured depth. The shorter depth and the lack of a deviation angle affected the pressure and enthalpy drop as the fluid rose to the top of the wellbore. The simulated profiles were sensitive to fluid enthalpy and the presence of non-condensable gases (Ambastha and Gudmundsson, 1986a). The Orkiszewski correlation was also found to be less reliable under the slug flow regime, which is the dominant flow regime in the Tanawon wells (Ambastha and Gudmundsson, 1986b). It must be stressed that pressure drop as the fluid rises from the bottommost feedzone is an important consideration when dealing with the calibration of multi-feed wellbores in HOLA. Feedzones in HOLA are characterized by productivity indices so that the mass flow contribution of the shallower feedzones is dependent on the pressure of the fluid at that depth. For the same productivity index, a lower pressure drop from the bottom will result in a lower contribution at the shallower feedzone. In terms of calibration, this may result in unnecessarily increasing the productivity index at the shallow feedzone to get the appropriate feedzone contribution.

### 5. LUMPED PARAMETER MODELLING OF PRESSURE MONITORING DATA

To get an analytic solution for the pressure response of the reservoir to the extraction at Tanawon sector, LUMPFIT was used to find an appropriate lumped parameter model for the pressure monitoring data of Well TW-3DA. As there was missing data in the middle of the data set due to the replacement of the pressure monitoring tool, the data before the 110th day were excluded from the modelling process to prevent LUMPFIT from interpolating production history within the gap. However, data from day 1 were loaded into LUMPFIT so that the corresponding production history would be considered in the modelling process. The dataset from the later part of the test was favoured because it has more data points and included the pressure response to the shutdown of Tanawon.

Modelling the pressure response against Tanawon extraction produced good matches indicating that the extraction in the Tanawon production area is well correlated with the pressure in Well TW-3DA. For the different Tanawon extraction models, the change in the fit is marginal as can be seen by the nearly overlapping plots in Figure 10. This insensitivity to the number of tanks can be attributed to very small conductivity values which means the production tank is not well connected to its surroundings. The main difference between the one- and two-tank models is that the two-tank model is more sensitive to fluctuations in production.

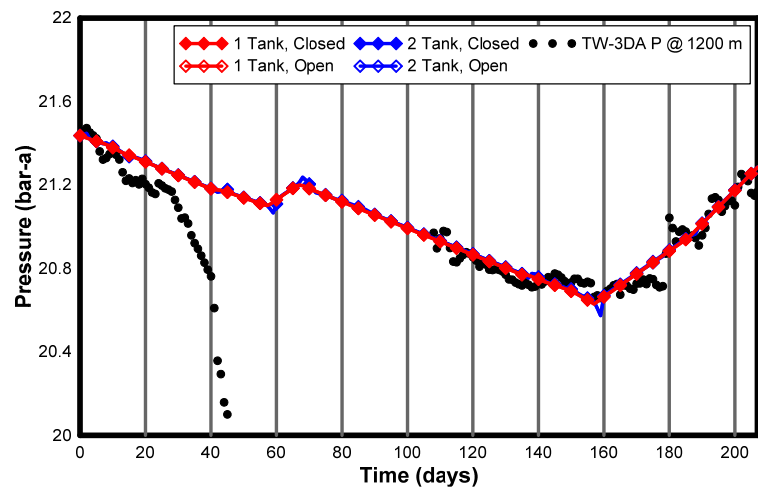


FIGURE 10: LUMPFIT model using Tanawon extraction against monitoring data

While the general drawdown and recovery trends are well represented by the Tanawon extraction model, there are portions of the data that cannot be explained by Tanawon extraction alone, which is an indication that there are other processes in the field affecting the pressure response in Well TW-3DA. Suspected, of course, is the extraction in the Cawayan sector.

The pressure cannot be modelled using Cawayan extraction alone because at the time of the pressure recovery, Cawayan extraction was constant. But by adding Cawayan extraction to Tanawon extraction (Figure 11), two features of the pressure response were better reflected by the model. The curvature of the drawdown while Tanawon was at maximum extraction was better matched and the change in slope due to the increase in Cawayan discharge was mimicked, though not matched. The pressure recovery was not as well captured as in the Tanawon extraction only model, because the step decrease around day 179 due to the shutdown of two of the wells was a smaller percentage of the total extraction. This increase in Cawayan production could also be attributed to the shutdown of Tanawon. In the Cawayan plus Tanawon extraction model, there were also marginal

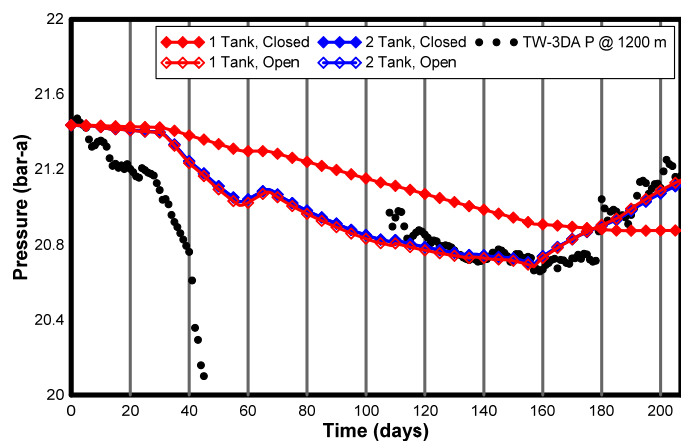


FIGURE 11: LUMPFIT model using Tanawon+Cawayan extraction against monitoring

differences between the one-tank, open and two-tank models. The recovery and drawdown of the two-tank models were slightly slower than that of the one-tank, open model. The one-tank, closed model was unable to match the recovery which is an indication that there is recharge coming into the area. Most likely due to the short duration of the test, it is unclear whether this recharge is merely from the periphery of the reservoir like from the second tank of a two tank model or true recharge from a constant pressure source.

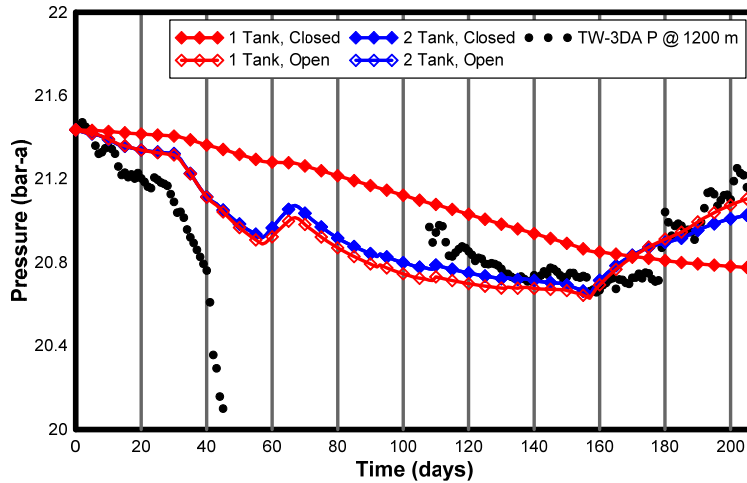


FIGURE 12: LUMPFIT model using Tanawon+Cawayan net extraction against monitoring

The last scenario considered was the scenario wherein the pressure response is influenced by injection in the area; however, when reinjection was considered, the matches did not improve (Figure 12). This does not mean that reinjection does not affect the monitoring well; rather, the effects of reinjection are not as strongly felt or not as immediately observed in the monitoring well.

The strong relationship between the pressure response in Tanawon and the extraction in Cawayan suggests that north to south may be the dominant flow direction. The seemingly weak correlation of

Tanawon with the Cawayan + Tanawon reinjection, on the other hand, points towards the idea that the NW to SE trending flow that would have been driven by the Pocdol belt may be a less prominent process. It is also possible that because the reinjection sector is a bit further away from the monitoring well than the Cawayan production area, the effects of reinjection have not yet been observed.

Looking at the statistical measures of fit given by LUMPFIT, the best fitting model was the one that utilizes Tanawon extraction on its own; however, in terms of capturing features of the pressure response, the Tanawon combined with the Cawayan extraction without injection was better. This illustrates that despite the statistical measures provided by LUMPFIT, it is still important to plot the results and examine whether they make sense. Table 1 summarizes the LUMPFIT parameters used for the best-fitting models.

TABLE 1: LUMPFIT parameters

Production data used	Model		A1	L1	A2	L2	B
	No. tanks	Boundary					
Tanawon Extraction	1	Closed	-	-	-	-	16.68
	1	Open	16.69	0.21E-05	-	-	0.00
	2	Closed	16.39	0.46E-06	-	-	0.16
	2	Open	16.39	0.46E-06	0.16	0.46E-07	0.00
Tanawon and Cawayan Total Extraction	1	Closed	-	-	-	-	4.10
	1	Open	18.21	0.24E-01	-	-	0.00
	2	Closed	16.94	0.23E-01	-	-	0.18
Tanawon and Cawayan Total Net Extraction	2	Open	16.94	0.23E-01	0.18	0.13E-02	0.00
	1	Closed	-	-	-	-	12.66
	1	Open	84.73	0.39E-01	-	-	0.00
	2	Closed	86.73	0.59E-01	-	-	4.50
	2	Open	90.73	0.59E-01	4.50	0.74E-03	0.00



Because the one- and two-tank, open models have almost the same results, the one-tank, open model may be selected as representative of this system. These results differ from the results of Fajardo (2000), which models the Cawayan area as a two-tank, open model. However, the complexity of the applicable lumped parameter model is known to be dependent on the length of time covered by the monitoring data (Axelsson, et al., 2005) and, so, the test duration may have the effect that the second tank is not yet clearly observable. The difference in best-fitting models may also be due to the difference in the location of the monitoring wells. The choice of monitoring wells that is able to represent the processes in the geothermal system of interest is important to the modelling process (Sarak et al., 2005). Fajardo's monitoring well, Pal-7D, is located close to the central production area and directed towards Cawayan sector, making it a good monitoring well for Cawayan. Based on the results of the lumped parameter modelling in this study, the Tanawon monitoring well is isolated from most external reservoir processes and is, thus, able to capture the response of the Tanawon reservoir to the simultaneous discharge test more clearly with less interference from the main production area.

Table 2: LUMPFIT parameters for model with turbulence

Production data used	Model		Turbulence coefficient	A1	L1	A2	L2	B
	No. tanks	Boundary						
Tanawon and Cawayan Total Extraction	2	Closed	0	16.94	0.23E-01	-	-	0.18
		Open		16.94	0.23E-01	0.18	0.13E-02	0.00
	2	Closed	0.35	26.50	0.32E-01	-	-	0.27
		Open		27.50	0.32E-01	0.55	0.96E-01	0.00

The model can be further improved by changing the turbulence coefficient (Table 2, Figure 13), which would normally be used to correct the pressure response of the well for skin losses close to the wellbore due to turbulence resulting from the sudden decrease in the effective flow cross-section from the reservoir to the wellbore. The effect of the turbulence can be observed in the relationship between the mass flow entering a feedzone  $Q$  and the difference between the reservoir pressure and the wellbore pressure at the feedzone. The expected behaviour for laminar flow is linear as characterized by the first-degree term in  $Q$  and coefficient,  $A$ . The turbulent effects are expressed by the squared term and coefficient,  $B$ . Note that when  $B = 0$ ,  $A$  is equivalent to the productivity index,  $PI$ .

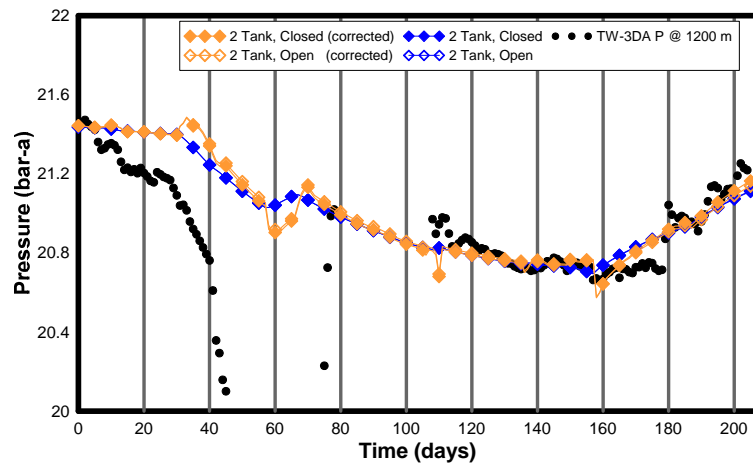


FIGURE 13: LUMPFIT model using Tanawon+Cawayan extraction with turbulence

The expected behaviour for laminar flow is linear as characterized by the first-degree term in  $Q$  and coefficient,  $A$ . The turbulent effects are expressed by the squared term and coefficient,  $B$ . Note that when  $B = 0$ ,  $A$  is equivalent to the productivity index,  $PI$ .

$$p_{reservoir} - p_{well@FZ} = AQ + BQ^2 \quad (3)$$

Because the monitoring well was not being discharged during the test, the turbulence effect could not be quantified. For purposes of this study, it was just an additional parameter to adjust in order to improve the model fit.

A cursory validation of the models can be done using idealized storage conditions for liquid reservoirs. The reservoir is known to have a two-phase cap based on the discharge of the wells, thus a free surface model was used. Table 3 summarizes the tank and fluid conductor properties from the first tank of the two-tank open models and the corresponding calculated areas.

Table 3: LUMPFIT-derived properties

Model	$\kappa_1$ (kg/Pa)	$\sigma_1$ (kg/s-Pa)	$A_{\text{free}}$ (km <sup>2</sup> )
Tanawon extraction (2-tank, open)	5176.60	0.12E-06	1.02
Tanawon + Cawayan extraction (2-tank, open)	5046.73	0.13E-02	0.99
Tanawon + Cawayan extraction with turbulence (2-tank, open)	3080.21	0.32E-01	0.60

The calculated areas are smaller than the actual assessment for Tanawon based on combined geoscientific and well testing data. Sarak et al. (2005) and Axelsson (1989) enumerated the possible reasons why such a calculation might be unreliable. These include pressure response influences that were not considered in the modelling, the short production history used, problems with data accuracy, and the fact that the system is actually two-phase. Another thing to look at it is the possible weighting of the influences. Summing up the production and injection from the different sectors assumes that each sector has equal influence on the pressure response, which is rarely the case in such a heterogeneous system. Finally, the assumption of all production coming from a single tank may not be fully applicable in this situation because during the simultaneous discharge test, the rest of BacMan was not shut down or discharging at a constant rate. This extraction would most likely not fall within the “first tank”.

## 6. NUMERICAL SIMULATION OF THE SIMULTANEOUS DISCHARGE TEST

The main weakness of the lumped parameter modelling is that it ignores the spatial geometry of the geothermal system. While lumped parameter modelling can be reliable for gauging pressure drawdown, it cannot model many of the other phenomena in geothermal utilization that should be considered when looking at sustainable production. Distributed parameter modelling or numerical reservoir modelling is able to look at a wider range of parameters.

The simultaneous discharge test was modelled using an AUTOUGH2 program developed for BGPF. The test was modelled by programming the model to extract mass from the reservoir equivalent to the extraction during the test itself. It was then determined whether with this extraction the pressure response observed in TW-3DA could be simulated.

### 6.1 TOUGH and AUTOUGH

TOUGH and its current incarnation TOUGH2 is one of the programs available for numerical reservoir modelling. It is a member of the multi-phase, multi-component family of codes referred to as MULKOM that is being developed in the Lawrence Berkeley National Laboratory (LBNL) (Reeves, et al., 1994). The name TOUGH is an acronym for “transport of unsaturated groundwater and heat” and was developed for problems that involve “strongly” heat-driven flow that is an effect of vaporization taking place at high water temperatures (Pruess, 1987). TOUGH2 was developed to extend the capabilities of TOUGH and was set up in such a way that future developments to the code would be encouraged (Reeves, et al., 1994). AUTOUGH2 is one of the customized versions of TOUGH2, developed by the University of Auckland. The main thrusts of the AUTOUGH2 development are to improve ease of use, increase execution speed, and extend TOUGH2 capabilities and options (Yeh et al., 2012).

The main problem solved by TOUGH and all its subsequent versions is solving the mass and energy balance for every grid-block in the model. The form of the mass balance and energy balance equations for the  $n^{\text{th}}$  grid-block with volume  $V_n$  and surface area  $A_n$  is the same and is given by

$$\frac{d}{dt} \int_{V_n} M^{(k)} dv = \int_{A_n} \mathbf{F}^{(k)} \cdot \mathbf{n} d\Gamma + \int_{V_n} q^{(k)} dv \quad (4)$$

where  $k$  is the component of interest, which can be heat, water, air, and more;  $M$  is the accumulation term, which accounts for how much of a component is contained in the grid-block;  $\mathbf{F}$  is the flux term, which refers to the amount of each component passing through the surface of the grid-block; and  $q$  is a term which is applicable for blocks that are sources or sinks of heat or mass. The differential equation is solved in space via integral finite differences and time evolution is solved through a fully implicit finite difference scheme, which would ensure unconditional stability to the numerical solution (Pruess, 1987). The flow of the fluid is governed by a multiphase extension of Darcy's Law while heat flows via convection and conduction (Pruess, et al., 1999). TOUGH is distributed as a series of separate equations of state (EOS) modules, which all solve Equation 4, but for different sets of components (Pruess et al., 1999). In AUTOUGH2, all the EOS modules are compiled together and are run on a single executable. To run the correct module, in addition to standard TOUGH2 inputs, the simulator or EOS to be used can be specified at the beginning (Yeh et al., 2012).

One of the most noticeable extensions made in AUTOUGH2 is the addition of new generator types. Generators, or sinks and sources, in TOUGH2 (Pruess, et al., 1999) were enumerated as follows:

- HEAT generator to act as heat sources;
- Injection generators (COM1/WATE, COM2 to COMn) to act as mass sources;
- MASS generator, which injects or withdraws a fixed amount of mass from the source or sink block;
- Wells on DELiVerability (DELV) sink, which simulates the feedzone of a well and withdraws fluid from a block based on a given productivity index, a given fixed wellbore pressure, and the calculated block pressure using  $PI = Q/(p_{block} - p_{well@FZ})$ ; and
- F-type wells on deliverability sink, which like DELV simulates the feedzone of a well and withdraws fluid from the block based on a given productivity index and the calculated block pressure, but solves for the wellbore pressure based on a well table provided in a file. The F-type generator is useful for implicit coupling of wellbore simulators and TOUGH2.

The DELV and F-type generators are used in simulating wells with a fixed wellhead pressure, which is often the case when wells are utilized for power production. The DELV generator assumes that the wellbore pressure required to discharge at the set wellhead pressure will be constant throughout production, which is only applicable when wellbore geometry, mass flow produced, and enthalpy are held constant. On the other hand, the F-type generator calculates this required wellbore pressure using the provided well table based on a fixed wellhead pressure. The MASS generator is useful when simulating production history, where actual extraction is known. Because the actual mass extraction is provided, the pressures within and near the wellbore are not taken into consideration.

AUTOUGH2 incorporates most of the TOUGH2 generators and introduced new generators, mostly variations of the DELV generator of TOUGH2. The F-type well was replaced by WFLO, which retrieves a well table from a file called WFLO. The main difference between the F-type and WFLO wells is that only one WFLO file can be used per simulation while any number of F-type wells can be called. Another generator type in AUTOUGH2 that can be used in a way that is similar to the F-type well is the geothermal well on DELiVerability (DELG), which has two modes of operation. Either DELG can be used to model a time-varying productivity index by providing a table of times and productivity index values or to give a wellbore pressure against enthalpy table. The second mode of operation is similar to F-type except the mass flow is not included in the well table. There are other new generator types in AUTOUGH2 described in Yeh et al. (2012), but they will not be discussed here as this study only utilized MASS, DELV, and DELG.

## 6.2 The 2010 BGPF reservoir model

The base model used for this study is the BGPF 3D reservoir model developed by Villacorte, Colina and others in 2010 using the Petra Sim graphical interface for TOUGH2 (Colina et al., 2011). The model is a single-porosity model with a rectangular grid that spans a total area of 1677 km<sup>2</sup> and 37 layers. The total number of grid blocks utilized by the model is 85,100, with finer meshing at the centre where the production area is located. Two convective systems were included in the model (Colina et al., 2011). Of interest is the main BacMan production area, which is outlined in white in Figure 14.

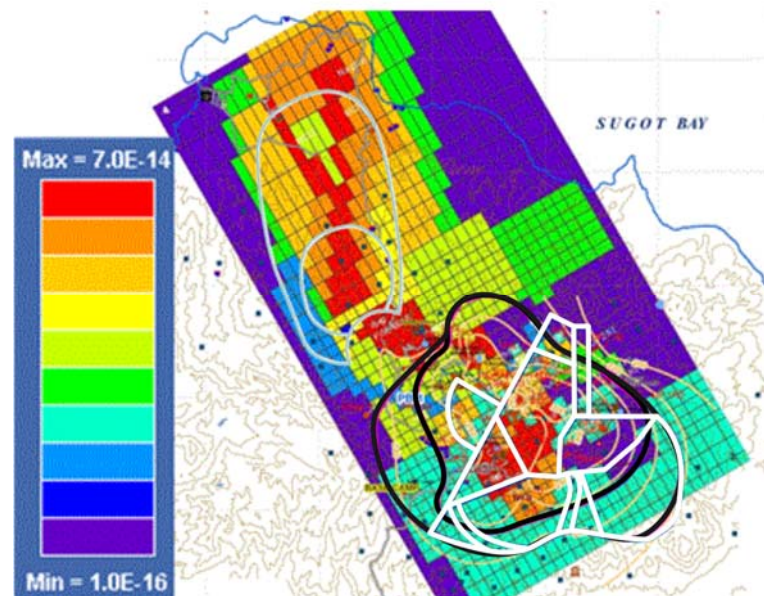


FIGURE 14: Permeability distribution at -1125mRSL (modified from Colina et al., 2011)

The model was calibrated against all available natural state temperatures and pressures in 2010 and over 17 years of production history. Production history data used were the discharge enthalpies of the wells and the pressure drawdown from 13 monitoring wells. Most wells in the field had good natural state temperature and pressure matches. The model was then converted to an AUTOUGH2 model for the simulation of CO<sub>2</sub> in the field. Profiles calibrated with CO<sub>2</sub> were similar to the profiles without CO<sub>2</sub> (Colina et al., 2011).

Two heat sources were used in the model, one for each of the modelled convective systems. The calibrated permeability distribution replicated the boundaries inferred from geophysical surveys (black lines in Figure 14). High permeability pathways were assigned towards the outflow regions (Colina et al., 2011).

At the time of the model's calibration, only Wells TW-1D and TW-2D had been drilled and neither had been produced for extended periods of time. While no Tanawon wells were used during the production history calibration of the model, four Cawayan wells were part of the calibration process. Enthalpy was not well matched in Cawayan with only two out of the four wells having a good match (Colina et al., 2011). The modelled pressure drawdown in Cawayan was also higher than the measured pressure drawdown.

During the model's development, Well TW-4D was included as a make-up well and its configuration did not include the perforated section, so a new sink was added to the model to include this feedzone.

## 6.3 Numerical simulation results

The time resolution needed to capture the pressure response during the simultaneous discharge test is fairly fine; however, if complex numerical models are being run, it is also not practical to impose a prohibitively small time step in order to create an "accurate" picture. Because Darcy is numerically stable when an implicit finite-differencing scheme is utilized, as it is in TOUGH2 and AUTOUGH (LBNL, 2013), the problem of large step sizes in the numerical model is not so much about achieving a stable solution, but more a problem of smoothing out fluctuations that should have otherwise been resolved by the model had a small time step been utilized. Using the fixed MASS model, three time

steps were tested and compared. The finest time step of 1.44E+5s (1.67 days) used was based on a maximum Courant number of 1. The Courant number is a stability criterion for numerical solutions to partial differential equations. Keeping the Courant number below 1 is a stability criterion for explicit finite difference schemes, and is, admittedly, too tight a restriction for TOUGH2. The largest time step of 2.59E+6 s is equivalent to one month. The third time step of 5.26E+5 s (6.1 days) was calculated based on the condition that the bulk fluid does not “skip over” blocks within one time step. The finer time steps are dependent on the average permeability in the area of interest. Mathematically, high permeability areas would require smaller stepping on account of faster breakthrough of fluids. Table 4 provides the details of the time step calculation.

The simulated pressure response was not compared with the actual pressure response using standard statistical regression methods because the monitoring block in the model is at a deeper depth than the actual monitoring depth within Well TW-3DA, resulting in a much higher pressure. While there is a block at the same depth as the pressure probe in the real monitoring well, the block is set within the caprock of the model, making it insensitive to the short-term changes induced by the simultaneous discharge test. The simulated pressure response is, therefore, only graphically compared with the actual pressure response.

Time step size does not affect the maximum pressure drop within the simulation period (Figure 15). The general trends of pressure lowering due to high extraction during the simultaneous discharge and recovery when the Tanawon wells were shut were all captured by the model regardless of the time step. The main feature that was smoothed out in the large time step was the recovery in pressure when Wells TW-1D and TW-4D were temporarily shut. A notable side effect of the fine time steps was that pressure recovery due to the shutdown of Tanawon occurred almost a full month earlier.

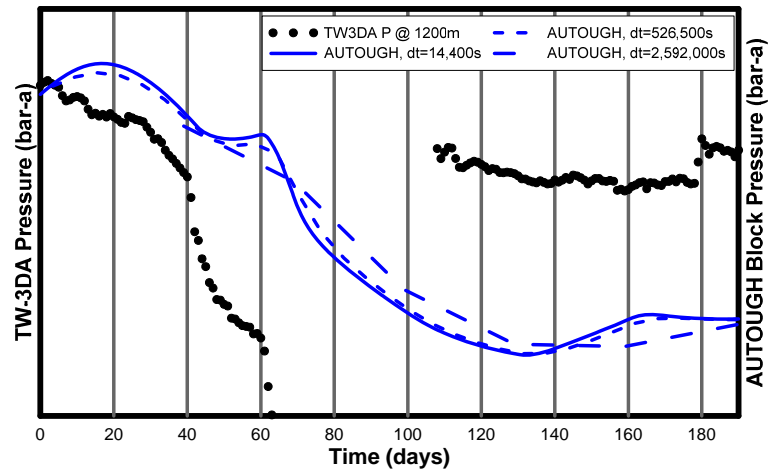


FIGURE 15: Comparison of fixed mass simulations with different time steps

This premature recovery is because AUTOUGH/TOUGH2 interpolated a linear decrease in production between full production and the shutdown period. AUTOUGH2 settings can be adjusted to remedy this. The initial pressure recovery at the beginning of the simulation can be related to changes in Cawayan production. It is unclear whether the real system responds in the same way due to the truncated data set. To balance between computational economy and time resolution, all other simulations utilized the 5.26E+5 s maximum time step.

TABLE 4: Comparison of time steps

Time step calculation	Time step (s)	No. of iterations	Minimum pressure (bar)
$C_{max} = 1 \geq \Delta t \left( \frac{u_x}{\Delta x} + \frac{u_y}{\Delta y} \right)$	14,400	1267	58.20
$\Delta t = \frac{\Delta x}{u_x}$	526,500	36	58.21
$\Delta t = 1 \text{ month}$	2,592,000	6	58.26

When compared against wells on DELV and the coupled model with wells on DELG, the wells discharging at predefined MASS followed the average monthly trend of the extraction as it was programmed to and hence followed the general pressure trends better but exhibited a larger drawdown than actually occurred (Figure 16). This is consistent with the observation regarding the pressure drawdown calibration for Cawayan. For the wells on DELV, the production was limited by the block pressure. The Tanawon blocks had pressures lower than what was actually measured in the reservoir, probably due to the simulated pressure drawdown in Cawayan being higher than actual. Because Cawayan is part of the flow path to Tanawon from the upflow, its pressures would affect the recharge in the Tanawon sector, as well. Thus, despite using the HOLA-simulated productivity index, the block pressures are too low to discharge at the same level as the real wells. For the wells on DELG, both enthalpy and block pressure affected the discharging conditions. The wells on DELG produced even less than the wells on DELV due to the enthalpy in the feed blocks being less than actual. Because of the low extraction in Tanawon in the DELV and DELG reservoir models, the pressure response in these models was dominated by extraction in other fields. Pressure recovery was not observed in either the DELV or DELG models. There was, however, a change in the pressure response slope at the point in time when the production in Tanawon was reduced, showing that the pressure monitoring block is not insensitive to Tanawon production and thus could be used as a monitoring block for forecasting.

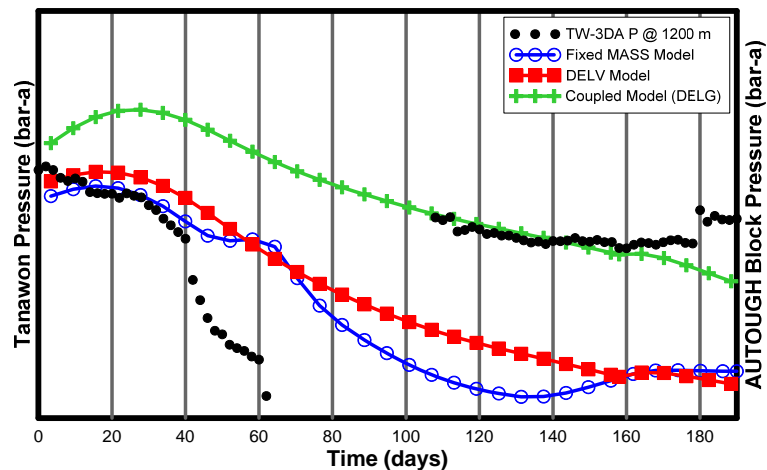


FIGURE 16: Comparison of simulations of the simultaneous discharge test using different sink types

## 7. LONG TERM FORECASTING

The purpose of long term forecasting is to gain a perspective on the impact of the different modelling schemes. Simulations for a ten-year production period were conducted and compared.

### 7.1 LUMPFIT forecasts

The ten-year forecast was performed assuming constant discharge for ten years at the level of the simultaneous discharge test maximum production. For Tanawon extraction models, the forecasts assumed that the field would be producing at the highest sustained production of Tanawon during the discharge test, while for the Tanawon + Cawayan extraction models, the forecasts assumed Tanawon extraction as detailed above plus the 20 MWe Cawayan production. Figure 17 shows a comparison of the different LUMPFIT forecasts.

The forecasts using Tanawon extraction models overlapped, all with linearly decreasing pressure, effectively acting like one-tank closed models. The addition of a second tank slightly reduced the drawdown rate, but the decay was still linear. The behaviour of the Tanawon extraction model forecasts can be attributed to low conductivity values.

Collectively, the forecast from the Tanawon extraction models can be seen as a pessimistic forecast, which disconnects the Tanawon reservoir from the rest of the BacMan resource. Given what is known

about the field and the results of other LUMPFIT models, this scenario is unlikely. The pessimistic models could not sustain the set discharge level for ten years. Negative pressures were calculated by year 7.

HOLA was used to determine at what date the wells would stop discharging at operating wellhead conditions. Figure 18 shows the bore output curves of the Tanawon wells. As drawdown increases, the output curves shift towards the left. It is apparent that the maximum discharge pressure of the wells decreased with increasing drawdown in the reservoir. Figure 17 shows that the higher enthalpy wells could tolerate significant drawdown, but the wells with liquid enthalpy could only discharge at the minimum operating wellhead pressure if drawdown stayed below 10.95 bar. Based on the rate of drawdown, low enthalpy wells like TW-2D can only be discharged for two years.

The forecasts using the Tanawon+Cawayan extraction on the other hand, suggest that the reservoir can sustain the combined production of the two fields for ten years. For the open and closed models, drawdown is negligible after a 1-bar pressure drop that occurs in the first year. Figure 17 shows that all wells can discharge under these conditions.

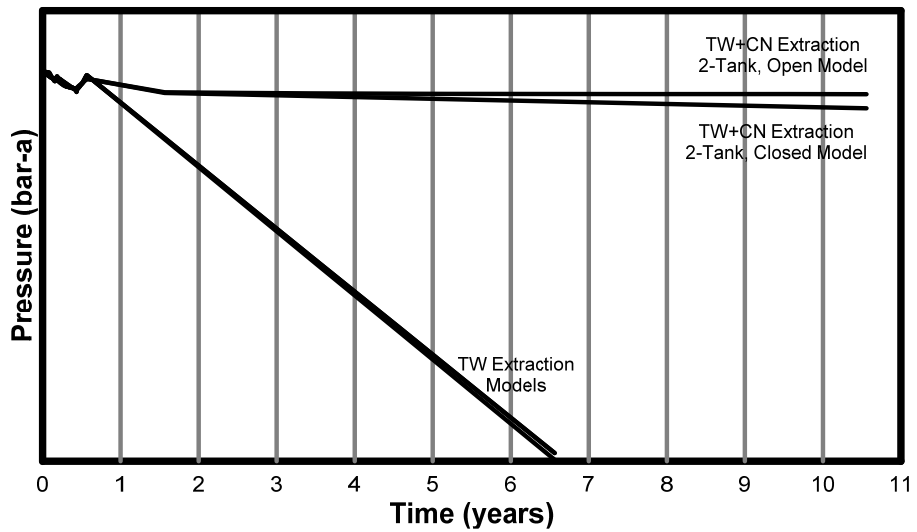


FIGURE 17: Comparison of LUMPFIT forecast results

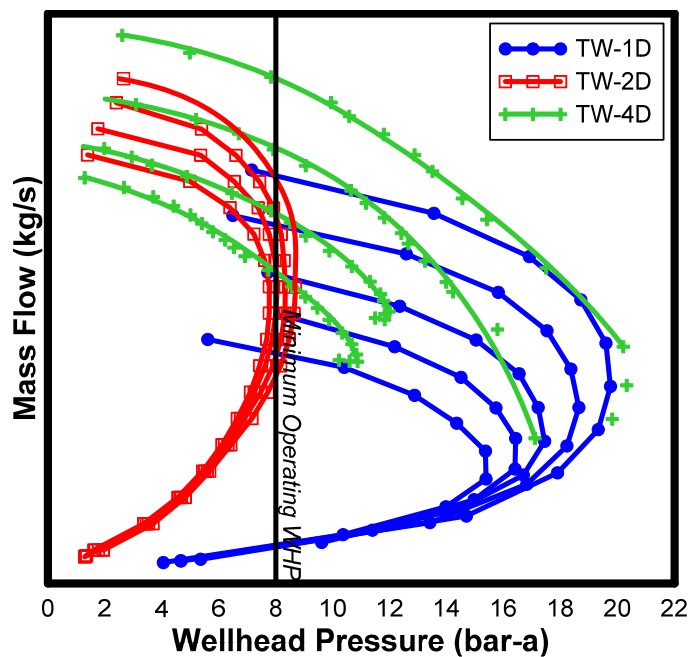


FIGURE 18: Bore output curves for varying reservoir pressure drawdown

Note that the basis for discharging was simply that the HOLA-calculated maximum discharge pressure be beyond the minimum operating wellhead pressure for the field. No changes were made to the wellbore configuration, which means it was assumed that there would be no scaling in the well. Scaling would reduce the flow diameter and increase friction losses as the fluid rises up the wellbore reducing the maximum discharge pressure for the same reservoir conditions. It was also assumed that the enthalpy would not change, which ignores boiling. Boiling would prolong the life of the well as higher enthalpy wells can keep discharging

### 7.2 Numerical model forecast

The effect of the different well types can only be seen with a simulation that covers a long period of time. Figure 19 illustrates the monitored pressure response for the various AUTOUGH2 models.

For fixed mass wells, the mass flows are based on the average production of the wells during the simultaneous discharge test. While the fixed mass well type produced results that most closely mimicked reality in the simulation of the simultaneous discharge test, it produced the most unrealistic results in the long term simulation. Blocks were forced to produce at a fixed rate regardless of block pressure, resulting in rapid drawdown. Before the second year of production, Well TW-1D began boiling due to over extraction while Well TW-4D enthalpies continuously rose beyond 3000 kJ/kg (Figure 20).

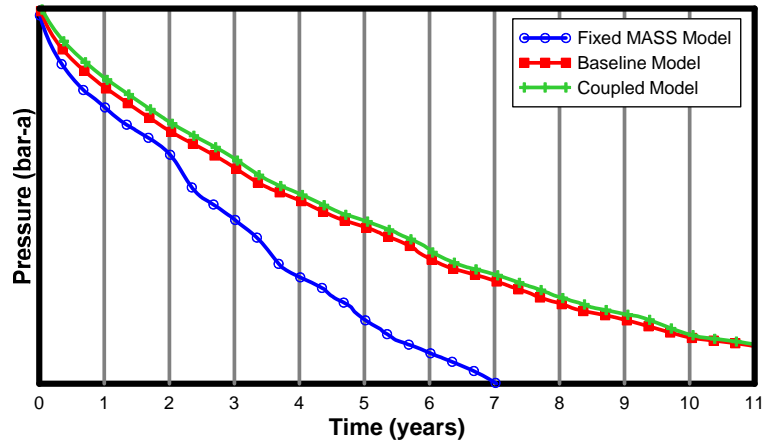


FIGURE 19: Comparison of AUTOUGH2 forecast results

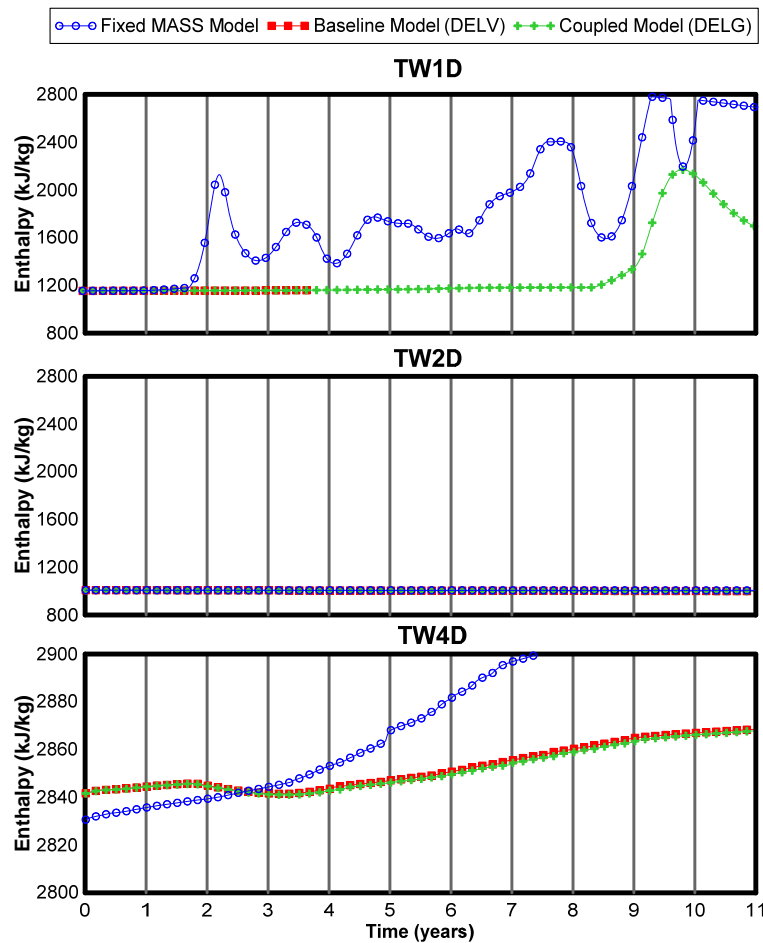


FIGURE 20: Discharge enthalpy trends for AUTOUGH2 forecasts

Tanawon, Well TW-1D became capable of production again. While the phenomenon of resurrecting Well TW-1D is not necessarily a realistic scenario, the capability of the coupled model to adjust its cut-

The baseline model used wells on DELV. This is more realistic than fixed MASS when it comes to simulation of production rates which are not yet available. In the baseline model, the blocks are not forced to produce more than what the reservoir is capable of discharging. If the block pressure is sustained, so is the level of production. The fixed wellbore pressure at depth acts as a cut-off pressure for production. If the block pressure drops below this cut-off pressure, then the well in the model stops discharging. In the baseline model, the cut-off pressure caused Well TW-1D to stop discharging before the fourth year. The coupled model, which uses wells on DELG, adjusted the cut-off pressure based on enthalpy. As illustrated in the bore output curves of Figure 18, higher enthalpy wells are more tolerant to drawdown. Because both the baseline model and the coupled model depend on a set productivity index, the two forecasts have similar behaviours in general. The main difference in the two models is that in the coupled model, when extraction created boiling in



off pressure based on the enthalpy of the discharge brings the simulation closer to a more accurate depiction of production.

From the perspective of the monitoring block, the difference between the baseline and the coupled model is negligible. However, the Tanawon wells are a small fraction of the total BacMan production so the effect of the coupling would not be as observable. Also, boiling in the area had just begun towards the end of the forecast; so the pressure response might deviate a bit more, further into the future.

### 7.3 Comparison of forecasts

In the long-term, the pressure drop in the AUTOUGH2 models agrees with the pressure drop simulated by LUMPFIT in the sense that the AUTOUGH2 simulated drawdown falls between the optimistic and pessimistic LUMPFIT forecasts. Figure 21 shows the comparison of the simulated pressure drawdown of the different forecast models.

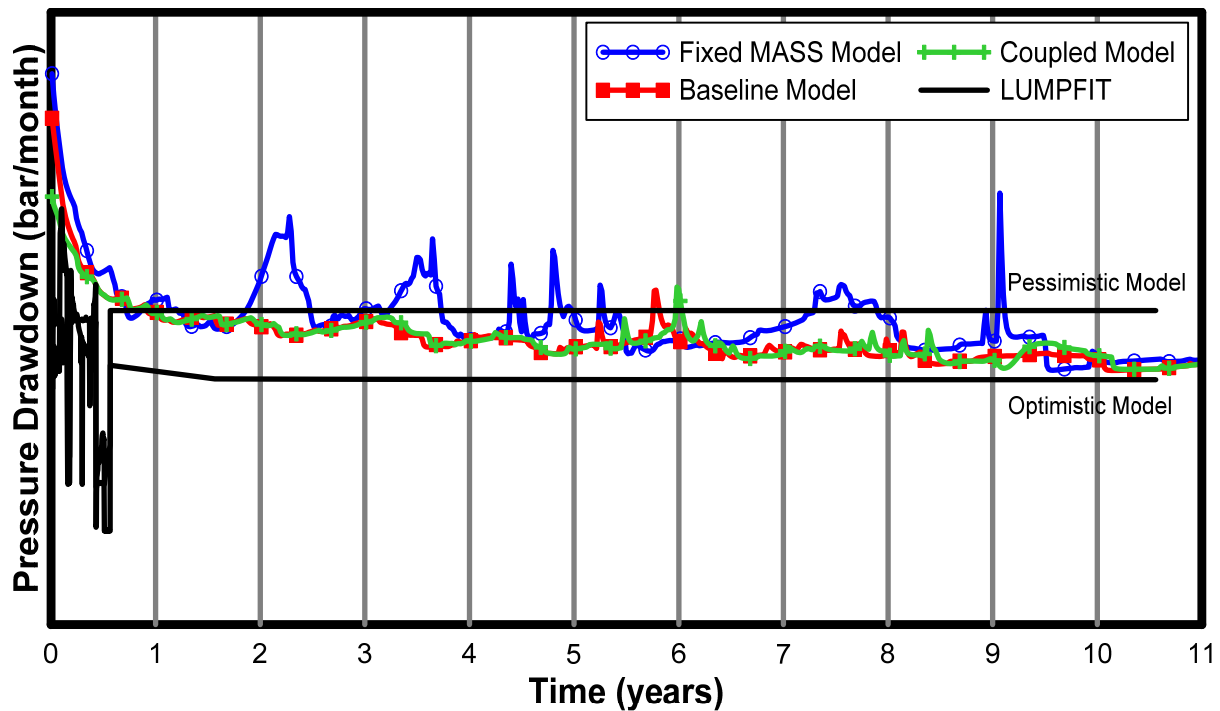


FIGURE 21: Comparison of pressure drawdown of different forecast models

It is expected that the LUMPFIT pessimistic model will always forecast the highest pressure drawdown, but this limit is crossed by the fixed MASS simulated drawdown, especially in the first four years of the forecast. Recall that based on wellbore simulations, Well TW-2D should stop discharging after two years if the pessimistic LUMPFIT drawdown applies. Since Figure 20 does not show any significant changes in Well TW-2D enthalpy, extraction in Well TW-2D should have stopped by the second year. But, since the fixed MASS simulation is blind to this, it keeps extracting via Well TW-2D, making the results of this simulation unfeasible.

On the other hand, the drawdown for the baseline and coupled models falls neatly between the optimistic and pessimistic LUMPFIT predicted drawdown. At the beginning of the forecast period, the AUTOUGH2 drawdown is comparable to the pessimistic model drawdown, but as the discharge of the wells is decreased by drawdown, the AUTOUGH2 drawdown falls closer to the LUMPFIT optimistic model drawdown.

## 8. SUMMARY

The Tanawon simultaneous discharge test and ten-year forecast were modelled using various methods and the model results and forecasts were compared. Simultaneous discharge testing was done to simulate production conditions and gain information about the field. The simultaneous discharge test data was analysed through LUMPFIT and AUTOUGH2 to look at the reservoir characteristics and through HOLA to examine wellbore characteristics. LUMPFIT was paired with HOLA simulations to determine whether the stable reservoir pressure would actually allow the wells to discharge. LUMPFIT was also paired with HOLA to find when the wells would stop discharging.

For the lumped parameter models, though the model ignores the spatial geometry of the reservoir, the relative influence of neighbouring fields could be gauged by modelling the pressure response with different extraction data. Because only drawdown is given by the lumped parameter model, wellbore simulators could be used to check whether the wells would still discharge given the calculated drawdown. This is especially important when wells in the area have an inherently low enthalpy or are affected by a cold recharge.

For the numerical models, coupling the model with a wellbore simulator extended the life of the wells that underwent boiling, but would stop low enthalpy wells from discharging earlier. In the 10 year forecast, the effect of coupling on the drawdown was negligible, though this was expected because coupling was only applied to a few of the wells whose cumulative output is a small fraction of the discharge from neighbouring fields. Because the coupled model is more sensitive to pressure drawdown and enthalpy than the baseline model, it is important that the reservoir model be recalibrated to get reasonable forecasts.

## ACKNOWLEDGEMENTS

I would like to extend my sincere gratitude to Mr. Lúdvík S. Georgsson for the opportunity to participate in the six-month training programme. To Dr. Ingvar Fridleifsson and all the other UNU-GTP lecturers who took time to mentor us and share with us their experiences in the geothermal industry, thank you and be assured that what you have invested in us is not for naught. To the UNU-GTP staff, Ingimar, Frída, Thórhildur, and Markús, who assisted and guided us through life in Iceland and made sure we got through the six months in one piece, no words can express how much your efforts are valued.

To my supervisors Ms. Sigrídur Sif Gylfadóttir and Dr. Andri Arnaldsson, this project would not have been completed had it not been for your direction and expertise. To my EDC supervisor, Sir Jericho Omagbon, thank you for sharing your ideas for the project and for always being there to check my work and encourage me. To my colleagues, Daryl Gamez, Christine Espartinez, Bryan Cacho, Thor Sazon, and Jeff Africa, thank you for sending me the data and references that I needed. Jefferson Villacorte and Raquel Colina, this project would not have been possible without your reservoir model. Thank you all very much for your patience with me.

Special thanks have to be extended to the management of the Energy Development Corporation, EDC President Richard Tantoco and TSS SVP Manny Ogena for not only allowing me to take part, but also for supporting me in this training programme. Sir Francis Sta. Ana, Sir Dave Yglopaz, and Sir Jericho, thank you for nominating me for this training.

To my family and my friends your love and prayers helped me pull through. *Ad majorem dei gloriam.*

## REFERENCES

- Ambastha, A.K., and Gudmundsson, J.S., 1986a: Pressure profiles in two-phase geothermal wells: comparison of field data and model calculations, *Proceedings of the 11<sup>th</sup> Workshop on Geothermal Reservoir Engineering, Stanford University, Stanford, Ca*, 183-188.
- Ambastha, A.K., and Gudmundsson, J.S., 1986b: Geothermal two-phase wellbore flow: pressure drop correlations and flow pattern transitions, *Proceedings of the 11<sup>th</sup> Workshop on Geothermal Reservoir Engineering, Stanford University, Stanford, Ca*, 277-281.
- Aragon A., Garcia, A., Baca, A., and Gonzáles, E., 1999: Comparison of measured and simulated pressure and temperature profiles in geothermal wells. *Geofísica Internacional*, 38-1, 35-42.
- Austria, J.J.C., 2008: *Production capacity assessment of the Bacon-Manito geothermal reservoir, Philippines*, University of Iceland, MSc thesis, UNU-GTP, Iceland, report 2, 62 pp.
- Axelsson, G., 1989: Simulation of pressure response data from geothermal reservoir by lumped parameter models. *Proceedings of the 14<sup>th</sup> Workshop on Geothermal Reservoir Engineering, Stanford University, California*, 257-263.
- Axelsson, G., 2013a: *Geothermal well testing*. UNU-GTP, Iceland, unpublished lecture notes.
- Axelsson, G., 2013b: *Dynamic modelling of geothermal systems*. UNU-GTP, unpublished lecture notes.
- Axelsson, G., and Arason, Th., 1992: *LUMPFIT, automated simulation of pressure changes in hydrological reservoirs. Version 3.1, user's guide*. Orkustofnun, Reykjavík, 32 pp.
- Axelsson, A., Björnsson, G., and Quijano, J.E., 2005: Reliability of lumped parameter modelling of pressure changes in geothermal reservoir. *Proceedings of the World Geothermal Congress 2005, Antalya, Turkey*, 8 pp.
- Bixley, P.F., 1988: Downhole measurements in geothermal wells. In: Okandan, E. (editor), *Geothermal reservoir engineering*. Kluwer Academic Publishers, Dordrecht, 41-53.
- Björnsson, G., 1987: *A multi-feedzone geothermal wellbore simulator*. Lawrence Berkeley Laboratory, report LBL-23546, 8-19.
- Braganza, J.S., 2011: *Geology of Bacon-Manito geothermal resource, resource assessment update of Bacon-Manito geothermal resource*. EDC internal report (unpublished), 66 pp.
- Colina, R.N., Villacorte, J.D., Ledesma, S.C., Omagbon, J.B., Austria, J.J.C., and Sta. Ana, F.X.M., 2011: *Update of the Bacon-Manito geothermal production field reservoir model*. EDC Resource Management, meeting report (unpublished), 15 pp.
- DOE, 2013: *Private sector initiated power projects*, Republic of the Philippines – Department of Energy, website, [www.doe.gov.ph/power-and-electrification/private-sector-initiated-power-projects](http://www.doe.gov.ph/power-and-electrification/private-sector-initiated-power-projects).
- EDC, 2003: *Environmental Impact Statement 50-80 MW Tanawon geothermal project (in Bacon-Manito geothermal production field)*, European Investment Bank, website, [www.eib.org/attachments/pipeline/20090372\\_eis\\_en.pdf](http://www.eib.org/attachments/pipeline/20090372_eis_en.pdf).
- EDC, 2013: *Our projects*. Energy Development Corporation, webpage, <http://www.energy.com.ph/our-projects/geothermal/>.

- Fajardo, V.R., 2000: Lumped parameter model of the Bacon-Manito geothermal production field, Albay, Philippines. *Proceedings of the World Geothermal Congress 2000, Kyushu-Tohoku, Japan*, 2551-2554.
- Fajardo, V.R., and Malate, R.C.M., 2005: Estimating the improvement of Tanawon production wells for acid treatment, Tanawon sector, BacMan geothermal production field, Philippines. *Proceedings of the World Geothermal Congress 2005, Antalya, Turkey*, 7 pp.
- Freeston, D., and Gunn, C., 1993: Wellbore simulation – case studies, *Proceedings of the 18<sup>th</sup> Workshop on Geothermal Reservoir Engineering, Stanford University, Stanford, California*, 261-266.
- Grant, M.A., 1982: A modified gas correction for the lip-pressure method, *Proceedings, 8<sup>th</sup> Workshop Geothermal reservoir engineering, Stanford University, Stanford, California*, 133-136.
- Grant, M.A., 1988: Reservoir physics and conceptual modelling. In: Okandan, E. (editor), *Geothermal reservoir engineering*. Kluwer Academic Publishers, Dordrecht, 23-40.
- Grant, M.A., 1997: Risk and resource assessment. *Proceedings of the PNOC-EDC 18<sup>th</sup> Geothermal Conference, Makati, Philippines*, 142-145.
- Gudmundsdóttir, H., 2012: *A coupled wellbore-reservoir simulator utilizing measured wellhead conditions*. University of Iceland, MSc thesis, Reykjavik, Iceland, 90 pp.
- Hsu, Y., and Graham, R.W., 1976: *Transport processes in boiling and two-phase systems*, Hemisphere Publishing Corporation, USA, 559 pp.
- Hu, B., Sagen, J., Chupin, G., Haugset, T., Ek, A., Sommersel, T., Xu, Z.G., and Mantecon, J.C., 2007: Integrated wellbore/reservoir dynamic simulation. *SPE Asia Pacific Oil & Gas Conference and Exhibition 2007, Jakarta, Indonesia*, 9 pp.
- IPGT, 2012: *Geothermal reservoir modelling*. International Partnership for Geothermal Technology, recommendations for research and development, August 2012, 25 pp.
- Liu Junrong, 2011: Well test interpretation and production prediction for well SD-01 in the Skarðdalur low-temperature field, Siglufjörður, N-Iceland. Report 19 in: *Geothermal training in Iceland 2011*. UNU-GTP, Iceland, 391-416.
- LBNL, 2013: *TOUGH2 software*. Lawrence Berkeley National Laboratory, Earth Sciences Division, website, [esd.lbl.gov/research/projects/tough/software/tough2.html](http://esd.lbl.gov/research/projects/tough/software/tough2.html).
- Malapitan, R.T and Reyes, A.N., 2000: Thermal areas of the Philippines. *Proceedings of the World Geothermal Congress 2000, Kyushu -Tohoku, Japan*, 1395-1400.
- Marcolini, M., and Batistelli, A., 2012: Modelling of wellbore flow within geothermal reservoir simulations at field scale. *Proceedings of the TOUGH Symposium 2012, Lawrence Berkeley National Laboratory, Berkeley, California*, 9 pp.
- Murray, L., and Gunn, C., 1993: Toward integrating geothermal reservoir and wellbore simulation: TETRAD and WELLSIM. *Proceedings of the 15<sup>th</sup> NZ Geothermal Workshop, Auckland*, 279-284.
- O’Sullivan, M.J., Pruess, K., Bodvarsson, G.S., and Lippmann, M.J., 2001: State of the art of geothermal reservoir simulation. *Geothermics*, 30-4, 395-429.

Pan, L., and Oldenburg, C.M., 2012: T2WELL – An integrated wellbore-reservoir simulator. *Proceedings of the TOUGH Symposium 2012, Lawrence Berkeley National Laboratory, Berkeley, California*, 8 pp.

Pruess, K., 1987: *TOUGH user's guide*. Lawrence Berkeley Laboratory, 73 pp.

Pruess, K., 2002: *Mathematical modeling of fluid flow and heat transfer in geothermal systems – an introduction in five lectures*. UNU-GTP, Iceland, report 3, 84 pp.

Pruess, K., 2003: Preface to TOUGH Symposium 2003, *Geothermics*, 33, 399-400.

Pruess, K., Oldenburg, C., and Moridis, G., 1999: *TOUGH2, user's guide version 2.0*. Lawrence Berkeley National Laboratory, 197 pp.

Pruett Tech Inc., 2013: *Pruett Tech Inc.* Pruet Tech Inc., website, <http://pruettech.com/>

Ramey, J.R., 1988: Transient pressure testing in geothermal reservoirs. In: Okandan, E. (editor), *Geothermal reservoir engineering*. Kluwer Academic Publishers, Dordrecht, 55-62.

Ramos, S.G., 2002: Potential constraints to the development of the Rangas sector based on petrologic evaluation of the BacMan geothermal field, Philippines. *Proceedings 27<sup>th</sup> Workshop on Geothermal Reservoir Engineering, Stanford University, Stanford, California*, 9 pp.

Ramos, S.G., and Santos, B.N.A., 2012: Updated hydrogeological model of the Bacon-Manito geothermal field, Philippines. *Proceedings of the 37th Workshop on Geothermal Reservoir Engineering, Stanford University, Stanford, Ca*, 4 pp.

Reeves, M., Baker, N.A., and Duguid, J.O., 1994: *Review and selection of unsaturated flow models*. Report prepared for US Department of Energy, Yucca Mountain Site Characterization Project, Las Vegas, Nevada.

Reyes, A.G., Zaide-Delfin, M.C., and Bueza, E.L., 1995: Petrological identification of multiple heat sources in the Bacon-Manito geothermal system, the Philippines. *Proceedings of the World Geothermal Congress 1995, Florence, Italy*, 2, 713-717.

Rivera A., M.A., 2000: *Coupled geothermal reservoir-wellbore simulation with a case study for the Námafjall field, N-Iceland*. University of Iceland, MSc thesis, UNU-GTP, Iceland, report 2, 74 pp.

Ruaya, J.R., Buenviaje, M.M., Solis, R.P., and Gonfiantini, R., 1994: *Chemical and isotopic studies of fluids in the Bacon-Manito geothermal field, Philippines*. IAEA-TECDOC Series, 185-209.

Sarak, H.E., Korkmaz, E.D., Onur M., and Satman A., 2005: Problems in the use of lumped-parameter reservoir models for low-temperature geothermal fields, *Proceedings of the World Geothermal Congress 2005, Antalya, Turkey*, 9 pp.

Sarmiento, Z.F., 1993: *Geothermal development in the Philippines*. UNU-GTP, report 2, 99 pp.

Tolentino, B.S., and Alcaraz, A.P., 1986: Strategies relating to the exploration and development of a geothermal field: A case for Bacon-Manito geothermal project, Albay/Sorsogon provinces Philippines. In: Tolentino, B. (lect.), *Lectures on geothermal energy in the Philippines*. UNU-GTP, Iceland, Report 12, 91-121.

Yeh, A., Croucher, A.E., and O'Sullivan, M.J., 2012: Recent developments in the AUTOUGH2 simulator, *Proceedings of the TOUGH Symposium 2012*. Lawrence Berkeley National Laboratory, Berkeley, California, 8 pp.

Yu, S., Ya-ju H., Bacolcol, T., Chia-Chu, Y., and Solidum, R., 2013: Present-day crustal deformation along the Philippine fault in Luzon, Philippines. *J. Asian Earth Sciences*, 65, 64-74.

Yumul, G.P., Dimalanta, C.B., Maglambayan, V.B., and Marquez, E.J., 2008: Tectonic setting of a composite terrain: A review of the Philippine island arc system. *Geosciences J.*, 12-1, 7-17.